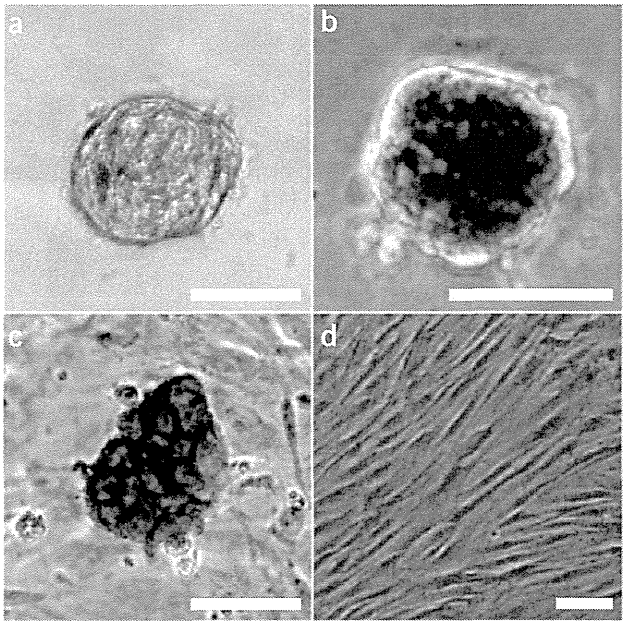

Figure 5 | Characterization of M-clusters. (**a**) Phase-contrast image of an M-cluster. (**b–d**) The result of the ALP reaction; the M-cluster (**b**) and mouse ES cells (**c**) are positive for the ALP reaction, whereas NHDFs (**d**) are negative. Scale bars, 50 μm (**a–c**), 100 μm (**d**).

Muse cells can be purified from the mesenchymal cell populations such as adult human BMSCs, dermal fibroblasts and the mononuclear cell population of fresh bone marrow by FACS using the antibody against the specific cell surface marker SSEA-3 (**Fig. 4**). The percentage of SSEA-3$^+$ cells among these cell populations is dependent on the cell sources: it is <1% in adult human cultured BMSCs, 2–3% in adult human cultured fibroblasts and 0.003–0.004% in mononuclear cells directly isolated from fresh bone marrow. Muse cells have telomerase activity as low as that of naive fibroblasts or BMSCs (**Supplementary Fig. 1**), suggesting low tumorigenicity of Muse cells. After SSEA-3$^+$ cells are isolated, they can be cultured in a single-cell suspension culture or an MC culture. About half (40–60%) of the Muse cells form M-clusters, whose diameters are >25 μm and which resemble embryoid bodies generated from human ES cells, have ALP activity similar to that of other pluripotent cells (**Fig. 5**) and contain the cells positive for pluripotency markers such as Nanog, Oct3/4 and Sox2 in addition to SSEA-3 (as shown by immunocytochemical analysis and RT-PCR (**Fig. 6**)). The growth curve of Muse cells in M-cluster formation shows the limitation of proliferative activity of Muse cells in a single-cell suspension culture (**Supplementary Fig. 2**). The proportion of M-cluster–forming activity is dependent on the viability of cells and is usually 45–65% in our laboratory. In contrast, SSEA-3$^-$ and/or CD105$^-$ cells did not form any clusters after single-cell suspension culture or MC culture. After expansion of M-clusters in adherent culture, second-generation M-cluster can be formed from the M-cluster-derived adherent culture–expanded cells, and the proportion of second-generation M-cluster formation is 48.0 ± 5.8% (fibroblasts) (mean ± s.d.) or 40.3 ± 9.1% (BMSCs). Alternatively, Muse cells can be isolated by FACS sorting with anti–SSEA-3 antibody, and the percentage of SSEA-3$^+$ cells is 45.0 ± 3.2% (fibroblasts). This SSEA-3$^+$ percentage is similar to the proportion of M-cluster-forming cells after adherent culture presented above, suggesting that SSEA-3$^+$ Muse cells have M-cluster-forming activity.

Differentiation of Muse cells can be confirmed by two methods: a spontaneous differentiation assay in which they are cultured on the gelatin-coated coverslip or induced differentiation of Muse cells into mesodermal-, endodermal- and ectodermal-lineage cells. After culturing on a gelatin-coated coverslip with 10% (vol/vol) FBS in α-MEM, Muse cells spontaneously differentiate into cells representative of all three germ layers, including cells positive for neurofilament (marker for neuronal cells, ectodermal lineage), SMA (smooth muscle, mesodermal lineage), α-fetoprotein (hepatocyte, endodermal lineage), cytokeratin-7 (biliary duct, endodermal lineage) and desmin (muscle, mesodermal lineage) (**Fig. 7a–d**). RT-PCR demonstrates the expression

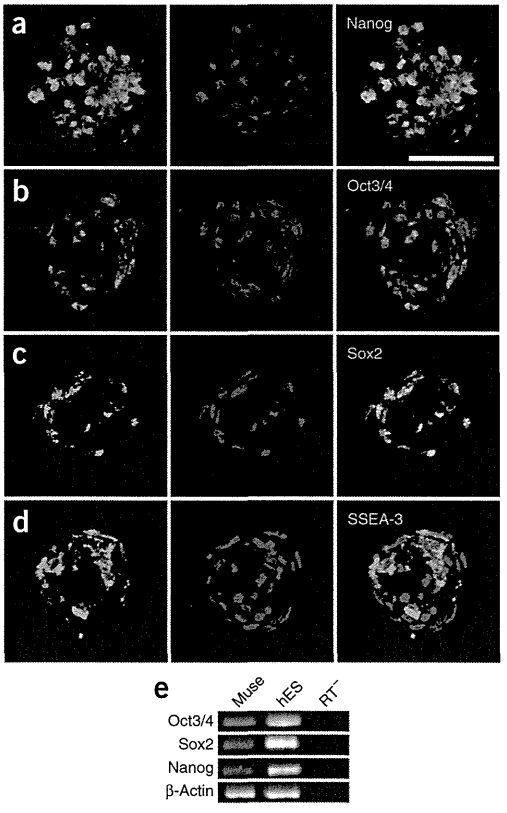

Figure 6 | Expression of pluripotency markers in M-clusters. (**a–d**) Immunocytochemical analysis showing cells in an M-cluster expressing pluripotency markers (green) such as Nanog (**a**), Oct3/4 (**b**), Sox2 (**c**) and SSEA-3 (**d**); nuclei are also visualized (blue). (**e**) mRNA expression of pluripotency markers. Human ES cells are used as a positive control. Scale bar, 50 μm. Samples treated without a reverse-transcription reaction (RT$^-$) are used as a negative control. Panels **a**,**b**,**e** are modified from Kuroda *et al.*[39], Wakao *et al.*[40] and Kuroda *et al.*[39], respectively.

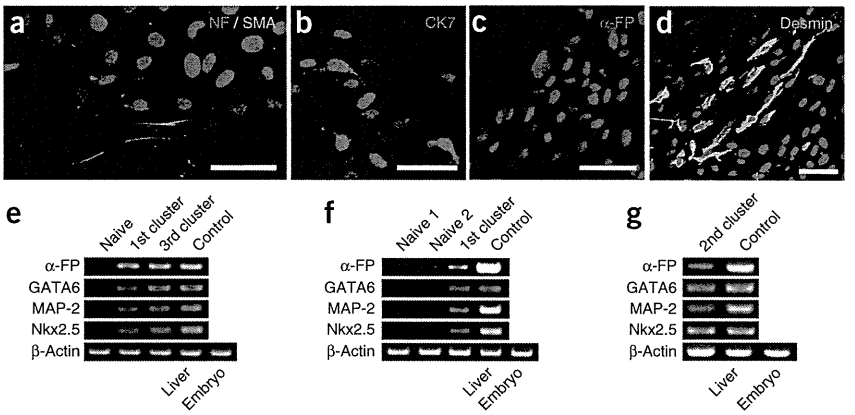

Figure 7 | Spontaneous differentiation of Muse cells on a gelatin-coated coverslip. (**a–d**) Immunocytochemistry against markers for specific cell types; M-cluster–derived cells cultured on gelatin-coated coverslips are positive for neurofilament NF and SMA (**a**), cytokeratin-7 (CK7) (**b**), α-fetoprotein (α-FP) (**c**) and desmin (**d**). (**e–g**) Expression of mRNA for cell lineage markers. M-cluster-derived cells cultured on the gelatin-coated coverslip express mRNA for α-FP, GATA6, MAP-2 and Nkx2.5 (**e**, cells from M-clusters derived from adult human dermal fibroblasts; (**f**,**g**) cells from M-clusters derived from a mononucleated cell of human fresh bone marrow). Human fetal liver (liver) was used as a positive control for α-FP, and whole human embryo (embryo) was used as a positive control for GATA6, MAP-2 and Nkx2.5. Scale bars, 50 μm. Panels **a**,**g** are modified from Wakao *et al.*[40] and Kuroda *et al.*[39], respectively.

of α-fetoprotein, GATA6 (endodermal lineage), MAP-2 (ectodermal lineage) and Nkx2.5 (mesodermal lineage) (**Fig. 7e–g**). Muse cells without induction of differentiation do not express any of the differentiation markers mentioned above, as shown by immunocytochemical analysis and RT-PCR (**Supplementary Fig. 3**).

The self-renewal property of Muse cells can be confirmed by cycle culture consisting of suspension culture–adherent culture–suspension culture. M-cluster in the third generation created by this cycle-culture method also has the same differentiation ability as that observed in the first generation (**Fig. 7e**), indicating the self-renewal property of Muse cells. Muse cells can differentiate into mesodermal-, endodermal- and ectodermal-lineage cells under the directed method. For example, Muse cells give rise to osteocalcin-positive osteocytes (**Fig. 8**) and adipocytes (mesodermal lineage) that are detected as cells containing lipid droplets inside the cytoplasm (**Fig. 8b**), and which are positive for oil red staining (**Fig. 8c**). These cells are representative of the mesodermal lineage. Hepatocytes (endodermal lineage) that express α-fetoprotein and human albumin are able to be produced from Muse cells after culturing with 10% (vol/vol) serum-containing medium supplemented with several hormones and trophic factors, including dexamethasone, HGF and FGF-4 (**Fig. 8d**,**i**). In the suspension culture system containing bFGF and EGF in a serum-free medium, Muse cells can also give rise to neural progenitor cells, which are positive for nestin (**Fig. 8e**), musashi-1 (**Fig. 8f**) and NeuroD (**Fig. 8g**) (ectodermal lineage). These neural progenitor cells differentiate into MAP-2$^+$ neurons upon treatment with bFGF and BDNF in adherent culture (**Fig. 8h**). These procedures confirm Muse cells' capacity for differentiation and self-renewal.

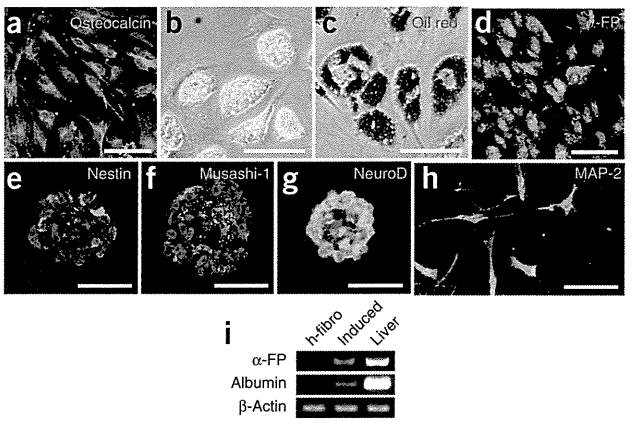

Figure 8 | Induced differentiation of Muse cells into mesodermal-, endodermal- and ectodermal-lineage cells. (**a–h**) Immunocytochemical analysis of differentiated cells. (**a**) After osteocyte induction, the cells positive for osteocalcin are detected. Adipocyte induction generates cells with lipid droplets (**b**) that are positive for oil red staining (**c**). (**d**) Hepatocyte induction generates cells positive for α-fetoprotein (α-FP). (**e–g**) After neural induction, the cells form spheres resembling neurospheres positive for the neural progenitor markers (green) Nestin (**e**), Musashi-1 (**f**) and NeuroD (**g**). (**h**) This neurosphere-like sphere gives rise to MAP-2$^+$ neurons after treatment with trophic factors. (**i**) mRNA expression in differentiated hepatocytes. M-cluster–derived cells (induced) can differentiate into cells expressing α-FP and human albumin mRNA, whereas naive adult human fibroblasts (h-fibro) do not express both mRNAs. Human fetal liver (liver) was used as a positive control. Scale bars, 50 μm (**a**,**d–h**), 20 μm (**b**,**c**).

Note: Supplementary information is available in the online version of the paper.

ACKNOWLEDGMENTS This work was supported by the Japan New Energy and Industrial Technology Development Organization. Antibodies against Oct3/4 were a gift from H. Hamada (Osaka University).

AUTHOR CONTRIBUTIONS Y.K., S.W., M.K. and M.D. contributed to the development of the methodology, Y.K., S.W., M.K., M.N. and M.D. performed the experiments and all the authors prepared the figures. M.K. and M.D. contributed to the description of the protocols.

COMPETING FINANCIAL INTERESTS The authors declare competing financial interests: details are available in the online version of the paper.

1. Gage, F.H. Mammalian neural stem cells. *Science* **287**, 1433–1438 (2000).
2. Weissman, I.L. & Shizuru, J.A. The origins of the identification and isolation of hematopoietic stem cells, and their capability to induce donor-specific transplantation tolerance and treat autoimmune diseases. *Blood* **112**, 3543–3553 (2008).
3. Kitada, M. & Dezawa, M. Induction system of neural and muscle lineage cells from bone marrow stromal cells; a new strategy for tissue reconstruction in degenerative diseases. *Histol. Histopathol.* **24**, 631–642 (2009).
4. Kuroda, Y., Kitada, M., Wakao, S. & Dezawa, M. Bone marrow mesenchymal cells: how do they contribute to tissue repair and are they really stem cells? *Arch. Immunol. Ther. Exp. (Warsz)* **59**, 369–378 (2011).
5. Pittenger, M.F. *et al.* Multilineage potential of adult human mesenchymal stem cells. *Science* **284**, 143–147 (1999).
6. Prockop, D.J. Marrow stromal cells as stem cells for nonhematopoietic tissues. *Science* **276**, 71–74 (1997).
7. Dezawa, M. *et al.* Bone marrow stromal cells generate muscle cells and repair muscle degeneration. *Science* **309**, 314–317 (2005).
8. Mizuno, H. *et al.* Myogenic differentiation by human processed lipoaspirate cells. *Plast. Reconstr. Surg.* **109**, 199–209, Discussion 210–211 (2002).
9. Wakitani, S., Saito, T. & Caplan, A.I. Myogenic cells derived from rat bone marrow mesenchymal stem cells exposed to 5-azacytidine. *Muscle Nerve* **18**, 1417–1426 (1995).
10. Makino, S. *et al.* Cardiomyocytes can be generated from marrow stromal cells *in vitro*. *J. Clin. Invest.* **103**, 697–705 (1999).
11. Rangappa, S., Entwistle, J.W., Wechsler, A.S. & Kresh, J.Y. Cardiomyocyte-mediated contact programs human mesenchymal stem cells to express cardiogenic phenotype. *J. Thorac. Cardiovasc. Surg.* **126**, 124–132 (2003).
12. Oswald, J. *et al.* Mesenchymal stem cells can be differentiated into endothelial cells *in vitro*. *Stem Cells* **22**, 377–384 (2004).
13. Cao, Y. *et al.* Human adipose tissue-derived stem cells differentiate into endothelial cells *in vitro* and improve postnatal neovascularization *in vivo*. *Biochem. Biophys. Res. Commun.* **332**, 370–379 (2005).
14. Dezawa, M. *et al.* Specific induction of neuronal cells from bone marrow stromal cells and application for autologous transplantation. *J. Clin. Invest.* **113**, 1701–1710 (2004).
15. Woodbury, D., Schwarz, E.J., Prockop, D.J. & Black, I.B. Adult rat and human bone marrow stromal cells differentiate into neurons. *J. Neurosci. Res.* **61**, 364–370 (2000).
16. Mimura, T., Dezawa, M., Kanno, H., Sawada, H. & Yamamoto, I. Peripheral nerve regeneration by transplantation of bone marrow stromal cell-derived Schwann cells in adult rats. *J. Neurosurg.* **101**, 806–812 (2004).
17. Dezawa, M., Takahashi, I., Esaki, M., Takano, M. & Sawada, H. Sciatic nerve regeneration in rats induced by transplantation of *in vitro*–differentiated bone-marrow stromal cells. *Eur. J. Neurosci.* **14**, 1771–1776 (2001).
18. Schwartz, R.E. *et al.* Multipotent adult progenitor cells from bone marrow differentiate into functional hepatocyte-like cells. *J. Clin. Invest.* **109**, 1291–1302 (2002).
19. Miyazaki, M. *et al.* Improved conditions to induce hepatocytes from rat bone marrow cells in culture. *Biochem. Biophys. Res. Commun.* **298**, 24–30 (2002).
20. Tang, D.Q. *et al. In vivo* and *in vitro* characterization of insulin-producing cells obtained from murine bone marrow. *Diabetes* **53**, 1721–1732 (2004).
21. Timper, K. *et al.* Human adipose tissue-derived mesenchymal stem cells differentiate into insulin, somatostatin, and glucagon expressing cells. *Biochem. Biophys. Res. Commun.* **341**, 1135–1140 (2006).
22. Ferrari, G. *et al.* Muscle regeneration by bone marrow-derived myogenic progenitors. *Science* **279**, 1528–1530 (1998).
23. Orlic, D. *et al.* Bone marrow cells regenerate infarcted myocardium. *Nature* **410**, 701–705 (2001).
24. Lee, J. *et al.* Migration and differentiation of nuclear fluorescence-labeled bone marrow stromal cells after transplantation into cerebral infarct and spinal cord injury in mice. *Neuropathology* **23**, 169–180 (2003).
25. Tomita, M. *et al.* Bone marrow-derived stem cells can differentiate into retinal cells in injured rat retina. *Stem Cells* **20**, 279–283 (2002).
26. Tamai, K. *et al.* PDGFRα-positive cells in bone marrow are mobilized by high mobility group box 1 (HMGB1) to regenerate injured epithelia. *Proc. Natl. Acad. Sci. USA* **108**, 6609–6614 (2011).
27. Sakaida, I. *et al.* Transplantation of bone marrow cells reduces CCl4-induced liver fibrosis in mice. *Hepatology* **40**, 1304–1311 (2004).
28. Zuk, P.A. *et al.* Human adipose tissue is a source of multipotent stem cells. *Mol. Biol. Cell* **13**, 4279–4295 (2002).
29. De Bari, C., Dell'Accio, F., Tylzanowski, P. & Luyten, F.P. Multipotent mesenchymal stem cells from adult human synovial membrane. *Arthritis Rheum.* **44**, 1928–1942 (2001).
30. Ishizeki, K., Nawa, T. & Sugawara, M. Calcification capacity of dental papilla mesenchymal cells transplanted in the isogenic mouse spleen. *Anat. Rec.* **226**, 279–287 (1990).
31. Kim, J.W. *et al.* Mesenchymal progenitor cells in the human umbilical cord. *Ann. Hematol.* **83**, 733–738 (2004).
32. Crigler, L. *et al.* Isolation of a mesenchymal cell population from murine dermis that contains progenitors of multiple cell lineages. *FASEB J.* **21**, 2050–2063 (2007).
33. Fuchs, E. & Segre, J.A. Stem cells: a new lease on life. *Cell* **100**, 143–155 (2000).
34. Hirata, T.M. *et al.* Expression of multiple stem cell markers in dental pulp cells cultured in serum-free media. *J. Endod.* **36**, 1139–1144 (2010).
35. Huang, H.I. *et al.* Multilineage differentiation potential of fibroblast-like stromal cells derived from human skin. *Tissue Eng. Part A* **16**, 1491–1501 (2010).
36. De Bari, C. *et al.* Mesenchymal multipotency of adult human periosteal cells demonstrated by single-cell lineage analysis. *Arthritis Rheum.* **54**, 1209–1221 (2006).
37. Sarugaser, R., Hanoun, L., Keating, A., Stanford, W.L. & Davies, J.E. Human mesenchymal stem cells self-renew and differentiate according to a deterministic hierarchy. *PLoS ONE* **4**, e6498 (2009).
38. Kitada, M. Mesenchymal cell populations: development of the induction systems for Schwann cells and neuronal cells and finding the unique stem cell population. *Anat. Sci. Int.* **87**, 24–44 (2012).
39. Kuroda, Y. *et al.* Unique multipotent cells in adult human mesenchymal cell populations. *Proc. Natl. Acad. Sci. USA* **107**, 8639–8643 (2010).
40. Wakao, S. *et al.* Multilineage-differentiating stress-enduring (Muse) cells are a primary source of induced pluripotent stem cells in human fibroblasts. *Proc. Natl. Acad. Sci. USA* **108**, 9875–9880 (2011).
41. Kucia, M. *et al.* A population of very small embryonic-like (VSEL) CXCR4$^+$SSEA-1$^+$Oct-4$^+$ stem cells identified in adult bone marrow. *Leukemia* **20**, 857–869 (2006).
42. Kucia, M., Wysoczynski, M., Ratajczak, J. & Ratajczak, M.Z. Identification of very small embryonic like (VSEL) stem cells in bone marrow. *Cell Tissue Res.* **331**, 125–134 (2008).
43. D'Ippolito, G. *et al.* Marrow-isolated adult multilineage inducible (MIAMI) cells, a unique population of postnatal young and old human cells with extensive expansion and differentiation potential. *J. Cell Sci.* **117**, 2971–2981 (2004).
44. Toma, J.G., McKenzie, I.A., Bagli, D. & Miller, F.D. Isolation and characterization of multipotent skin-derived precursors from human skin. *Stem Cells* **23**, 727–737 (2005).
45. De Kock, J., Vanhaecke, T., Biernaskie, J., Rogiers, V. & Snykers, S. Characterization and hepatic differentiation of skin-derived precursors from adult foreskin by sequential exposure to hepatogenic cytokines and growth factors reflecting liver development. *Toxicol. In Vitro* **23**, 1522–1527 (2009).
46. Bianco, P., Sacchetti, B. & Riminucci, M. Osteoprogenitors and the hematopoietic microenvironment. *Best Pract. Res. Clin. Haematol.* **24**, 37–47 (2011).
47. Sacchetti, B. *et al.* Self-renewing osteoprogenitors in bone marrow sinusoids can organize a hematopoietic microenvironment. *Cell* **131**, 324–336 (2007).

Functional Melanocytes Are Readily Reprogrammable from Multilineage-Differentiating Stress-Enduring (Muse) Cells, Distinct Stem Cells in Human Fibroblasts

Kenichiro Tsuchiyama[1,2], Shohei Wakao[2], Yasumasa Kuroda[3], Fumitaka Ogura[2], Makoto Nojima[2], Natsue Sawaya[1], Kenshi Yamasaki[1], Setsuya Aiba[1] and Mari Dezawa[2,3]

The induction of melanocytes from easily accessible stem cells has attracted attention for the treatment of melanocyte dysfunctions. We found that multilineage-differentiating stress-enduring (Muse) cells, a distinct stem cell type among human dermal fibroblasts, can be readily reprogrammed into functional melanocytes, whereas the remainder of the fibroblasts do not contribute to melanocyte differentiation. Muse cells can be isolated as cells positive for stage-specific embryonic antigen-3, a marker for undifferentiated human embryonic stem cells, and differentiate into cells representative of all three germ layers from a single cell, while also being nontumorigenic. The use of certain combinations of factors induces Muse cells to express melanocyte markers such as tyrosinase and microphthalmia-associated transcription factor and to show positivity for the 3,4-dihydroxy-L-phenylalanine reaction. When Muse cell–derived melanocytes were incorporated into three-dimensional (3D) cultured skin models, they localized themselves in the basal layer of the epidermis and produced melanin in the same manner as authentic melanocytes. They also maintained their melanin production even after the 3D cultured skin was transplanted to immunodeficient mice. This technique may be applicable to the efficient production of melanocytes from accessible human fibroblasts by using Muse cells, thereby contributing to autologous transplantation for melanocyte dysfunctions, such as vitiligo.

Journal of Investigative Dermatology (2013) **133,** 2425–2435; doi:10.1038/jid.2013.172; published online 16 May 2013

INTRODUCTION

Melanocytes produce melanin and deliver them to neighboring keratinocytes to protect the skin from UV rays (Slominski *et al.*, 2004; Kondo *et al.*, 2011). Melanocyte dysfunction results in a variety of pigment disorders, such as albinism and vitiligo, which cause not only cosmetic problems but also increase the risk of skin cancers due to incomplete protection from UV rays (Mabula *et al.*, 2012).

Current treatments for vitiligo include topical treatment with corticosteroids or immunomodulators, UV treatment, and autologous skin grafts (Alikhan *et al.*, 2011; Felsten *et al.*, 2011). The effectiveness of these treatments, however, is inadequate. Autologous cultured melanocyte transplantation is a potential cell therapy (van Geel *et al.*, 2001; Fioramonti *et al.*, 2012), but it is not widely used because human adult melanocytes are difficult to culture and amplify large scale *in vitro*. Several groups recently reported successful melanocyte induction from embryonic stem (ES) or induced pluripotent stem (iPS) cells (Yamane *et al.*, 1999; Fang *et al.*, 2006; Motohashi *et al.*, 2006; Nissan *et al.*, 2011; Ohta *et al.*, 2011; Yang *et al.*, 2011). Indeed, these are attractive cell sources for melanocyte induction, but the ethical problems in obtaining ES cells (Knoppers *et al.*, 2009; Manzar *et al.*, 2011) and the risk of tumorigenesis for both ES and iPS cells are obstacles to clinical use (Okita *et al.*, 2007; Fong *et al.*, 2010; Ben-David, 2011; Goldring *et al.*, 2011).

Mesenchymal stem cells (MSCs) are adult stem cells with a lower risk of tumorigenesis that exist in mesenchymal tissues, such as the bone marrow, dermis, fat tissue, and dental pulp, and are used for the treatment of many kinds of diseases (Macchiarini *et al.*, 2008; Hare *et al.*, 2009; Jiang *et al.*, 2011; Sng *et al.*, 2012). MSCs have attracted attention because of their ability to differentiate into a broad spectrum of cells.

[1]*Department of Dermatology, Tohoku University Graduate School of Medicine, Sendai, Miyagi, Japan;* [2]*Department of Stem Cell Biology and Histology, Tohoku University Graduate School of Medicine, Sendai, Miyagi, Japan and* [3]*Department of Anthropology and Anatomy, Tohoku University Graduate School of Medicine, Sendai, Miyagi, Japan*

Correspondence: Kenichiro Tsuchiyama, Department of Dermatology, Tohoku University Graduate School of Medicine, 1-1 Seiryo-machi, Aoba-ku, Sendai, Miyagi 980-8574, Japan. E-mail: tutiviola@med.tohoku.ac.jp or Mari Dezawa, Department of Stem Cell Biology and Histology and Department of Anthropology and Anatomy, Tohoku University Graduate School of Medicine, 2-1 Seiryo-machi, Aoba-ku, Sendai, Miyagi 980-8575, Japan. E-mail: mdezawa@med.tohoku.ac.jp

Abbreviations: 3D, three dimensional; DCT, dopachrome tautomerase; DPSC, dental pulp stem cell; ES, embryonic stem; ET-3, endothelin-3; GFP, green fluorescent protein; iPS, induced pluripotent stem; L-DOPA, 3,4-dihydroxy-L-phenylalanine; MITF, microphthalmia-associated transcription factor; MSC, mesenchymal stem cell; Muse, multilineage-differentiating stress-enduring; NHDF, normal human dermal fibroblast; RT–PCR, reverse transcription–PCR; SCF, stem cell factor; SKP, skin-derived precursor cell; SSEA-3, stage-specific embryonic antigen-3; TRP-1, tyrosinase-related protein 1

Received 8 November 2012; revised 5 March 2013; accepted 11 March 2013; accepted article preview online 5 April 2013; published online 16 May 2013

MSCs can differentiate not only into mesodermal lineage cells but also into ectodermal or endodermal lineage cells (Pittenger *et al.*, 1999; Dezawa *et al.*, 2004; Sakaida *et al.*, 2004; Phinney *et al.*, 2007). Melanocytes have also been induced from dental pulp stem cells (DPSCs) (Stevens *et al.*, 2008; Paino *et al.*, 2010) However, MSCs generally comprise crude cell populations and contain different cell types on the basis of their cell surface antigens because they are usually harvested just as adherent cells from mesenchymal tissues. Therefore, the cells responsible for differentiation across the oligolineage boundaries between the mesoderm and the ectoderm, namely mesenchymal to melanocytes, remain unknown.

We recently reported a type of stem cell that exists among adult human MSCs that we named multilineage-differentiating stress-enduring cells (Muse cells) (Kuroda *et al.*, 2010; Wakao *et al.*, 2011). Muse cells normally exist in human mesenchymal cultured cells, such as dermal fibroblasts and bone marrow stromal cells, and also in mesenchymal tissue, such as dermis and bone marrow. Muse cells have characteristics similar to both pluripotent stem cells and MSCs: they can be isolated by FACS as cells double positive for pluripotency (stage-specific embryonic antigen-3 (SSEA-3), a marker for undifferentiated human ES cells) and mesenchymal markers (CD105) and have the ability to self-renew and differentiate into endodermal-, mesodermal-, and ectodermal-lineage cells from a single cell. Unlike other pluripotent stem cells such as ES cells and iPS cells, however, Muse cells have low telomerase activity and do not form tumors *in vivo*. Thus, they have a high potential for clinical application. Recently, skin-derived precursor (SKPs) cells have been reported as multipotent MSCs in human foreskins (Toma *et al.*, 2005). However, unlike SKPs, Muse cells are located sparsely in the connective tissue of the dermis and the adipose tissue and are not associated with any particular structure such as dermal papilla, connective tissue sheath, or hair follicular epithelium. In addition, Muse cells do not express the SKP markers *Snail* and *Slug* (Wakao *et al.*, 2011). These data indicate that Muse cells are distinct from SKPs.

We recently discovered that Muse cells in human dermal fibroblasts are readily reprogrammed into functional melanocytes by using certain combinations of factors and cytokines. Muse cell–derived melanocytes (Muse melanocytes) expressed melanocyte markers such as microphthalmia-associated transcription factor (MITF), tyrosinase-related protein 1 (TRP-1), dopachrome tautomerase (DCT), KIT, gp100, and tyrosinase, and were positive for the 3,4-dihydroxy-L-phenylalanine (L-DOPA) reaction assay, produced melanin, and integrated into the basal layer of epidermis. In contrast, when the Muse cells were removed from human fibroblasts before melanocyte induction, the remaining cells (namely, "non-Muse cells") failed to become melanocytes and did not produce melanin. This finding indicates that Muse cells, the cells that already have triploblastic differentiation ability, can cross the oligolineage boundary between the mesodermal and ectodermal lineages and become reprogrammed into melanocytes, whereas the remaining fibroblasts do not participate in this event. Thus, Muse cells are an ideal cell source for generating functional melanocytes from adult human fibroblasts that can be applied to autologous transplantation for pigment disorders.

RESULTS

Isolation of Muse cells from human fibroblasts

Muse cells were collected from normal human dermal fibroblasts (NHDFs; Lonza Walkersville, MD). Because 100% of SSEA-3-positive cells from NHDF are positive for CD105, as described previously (Kuroda *et al.*, 2010), we isolated Muse cells by FACS as SSEA-3-positive cells. The ratio of SSEA-3-positive cells in NHDFs was in the range of 2 to 3%, consistent with the previous reports (Figure 1a).

We evaluated the differentiation ability of the collected Muse cells. When each Muse cell was cultured in a single-cell suspension culture after limiting dilution, cell clusters very similar to ES cell–derived embryoid bodies, namely Muse cell–derived cell clusters (M-clusters), were generated by day 7 (Figure 1b). These clusters were positive for alkaline phosphatase staining (Figure 1c); they expressed pluripotency markers such as Nanog, Oct 3/4, and Sox2; and they could self-renew, as reported previously (data not shown) (Wakao *et al.*, 2011). To observe their differentiation ability, single M-clusters were individually transferred onto gelatin-coated dishes. After 7 days, spontaneous differentiation of the cells expanding from the M-cluster into cells positive for neurofilament (ectodermal marker), α-smooth muscle actin (mesodermal marker), and GATA4 (endodermal marker) were detected (Figures 1d-f). In contrast, non-Muse cells did not form clusters in a single-cell suspension culture, and therefore differentiation of non-Muse cells into endodermal-, mesodermal-, and ectodermal-lineage cells could not be observed. These results are consistent with our previous report (Wakao *et al.*, 2011).

Differentiation of Muse cells into melanocytes

NHDF was separated into Muse and non-Muse cells by FACS and both were cultured separately in a specific differentiation medium containing 10 factors: Wnt3a, stem cell factor (SCF), endothelin-3 (ET-3), basic fibroblast growth factor, linoleic acid, cholera toxin, L-ascorbic acid, 12-*O*-tetradecanoylphorbol 13-acetate, insulin–transferrin–selenium, and dexamethasone (Figure 1g). The morphology of the Muse cells began to change and cells with dendrites appeared within 3 weeks. Cell size was slightly reduced by 5 weeks, and by 6 weeks, the cells had morphology similar to that of human melanocytes (Figure 2a and b). However, such changes did not occur in non-Muse cells, and most of the non-Muse cell–derived cells remained fibroblast-like cells, even after 6 weeks of differentiation.

Characterization of Muse melanocytes

The expression of melanocyte-related markers was examined in Muse melanocytes and non-Muse cell–derived cells after 6 weeks of differentiation. Human melanocytes were used as a positive control. In reverse transcription–RT–PCR, cells induced from Muse cells expressed MITF, KIT, TRP-1, and gp100 at 3 weeks (Figure 3a). In addition, Muse cells

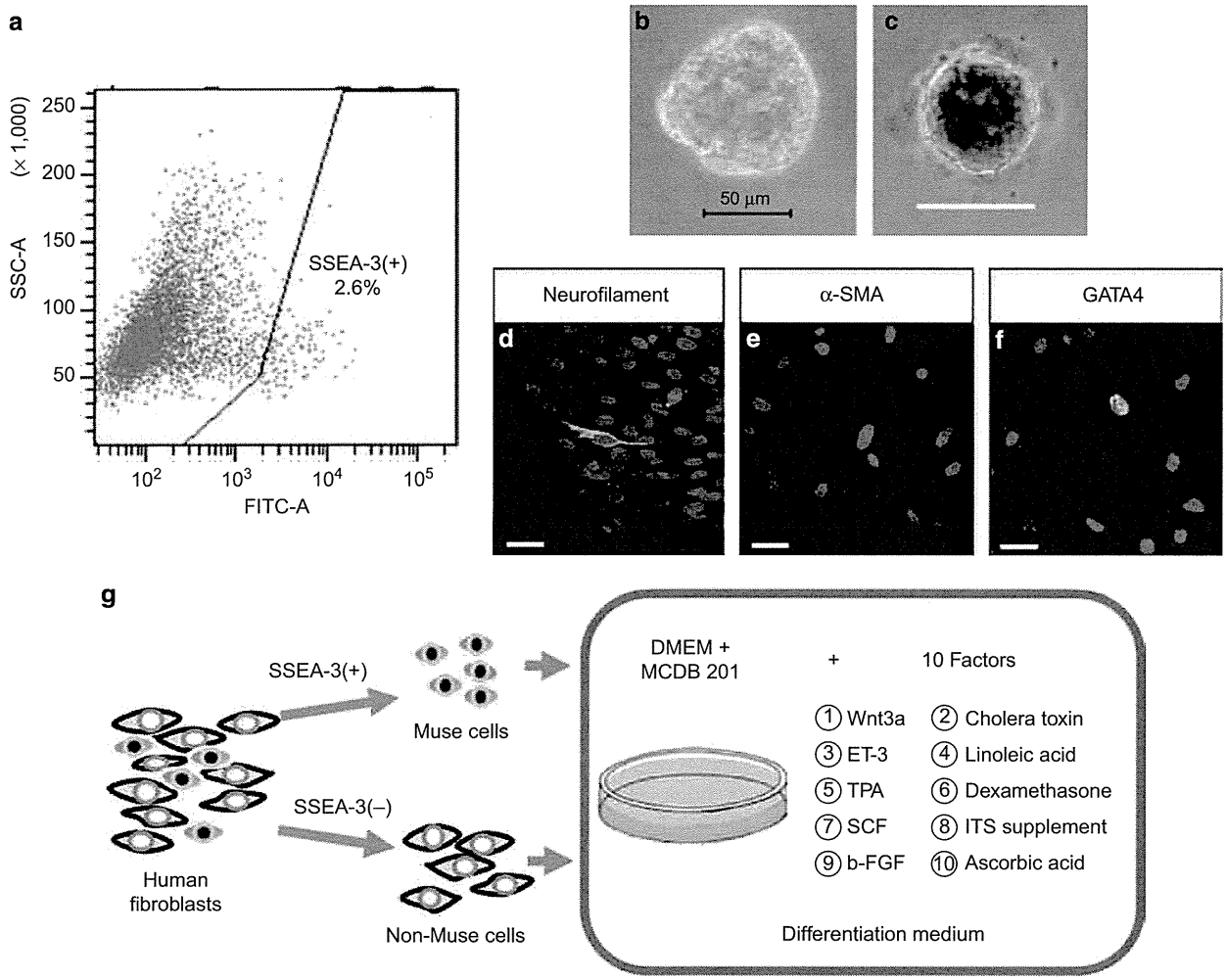

Figure 1. Characterization of Muse (multilineage-differentiating stress-enduring) cells. (**a**) FACS analysis for stage-specific embryonic antigen-3 (SSEA-3) expression in naive normal human dermal fibroblasts (NHDFs). (**b**) M-cluster formed in single-cell suspension culture at day 7. (**c**) Alkaline phosphatase (ALP) staining of an M-cluster. (**d–f**) Immunocytochemistry for (**d**) neurofilament, (**e**) α-smooth muscle actin (α-SMA), and (**f**) GATA4 in cells derived from a single M-cluster. (**g**) Schematic diagram of melanocyte differentiation from Muse cells and non-Muse cells. Scale bars = 50 μm (**b–f**). b-FGF, basic fibroblast growth factor; ET-3, endothelin-3; ITS, insulin–transferrin–selenium; SCF, stem cell factor; TPA, 12-*O*-tetradecanoyl-phorbol 13-acetate.

expressed DCT at 5 weeks and tyrosinase at 6 weeks. We previously reported that naive Muse cells do not express either DCT or TRP-1 (Wakao *et al.*, 2011); thus, the expression of these melanocyte-related markers in Muse cells is thought to be induced by differentiation. Although non-Muse cell–derived cells expressed MITF, KIT, and TRP-1 after 3 weeks, DCT, gp100, and tyrosinase were not expressed in these cells even after 6 weeks of differentiation (Figure 3a).

During immunocytochemical analysis, cells positive for tyrosinase, gp100, and MITF were detected in Muse melanocytes (6 weeks), as in the case of human melanocytes, whereas none of the cells positive for these melanocyte markers were observed in non-Muse cell–derived cells at the same time point (Figure 3b). Although an MITF signal was detected in non-Muse cell–derived cells in RT–PCR (Figure 3a), the protein expression level was not high enough to be detected by immunocytochemistry.

Muse melanocytes were further evaluated by the L-DOPA reaction assay to examine melanin productivity. Many cells were positive for the L-DOPA reaction assay (Figure 3c). These results suggested that cells with characteristics similar to those of human melanocytes were induced from Muse cells but not from non-Muse cells.

Effect of factors on melanocyte differentiation

To investigate the factors essential for melanocyte induction and to estimate whether the number of factors could be reduced from 10, 7 combinations of factors were created (Figure 4a). Muse cells cultured in media 1, 2, 3, 4, and 7 grew well, but they did not become similar to authentic human melanocytes. Muse cells cultured in media 5 and 6 did not proliferate well and all of them died within 20 days (Figure 4a and c). RT–PCR analysis revealed no expression of tyrosinase in all 7 sets of medium at 6 weeks, and thus these

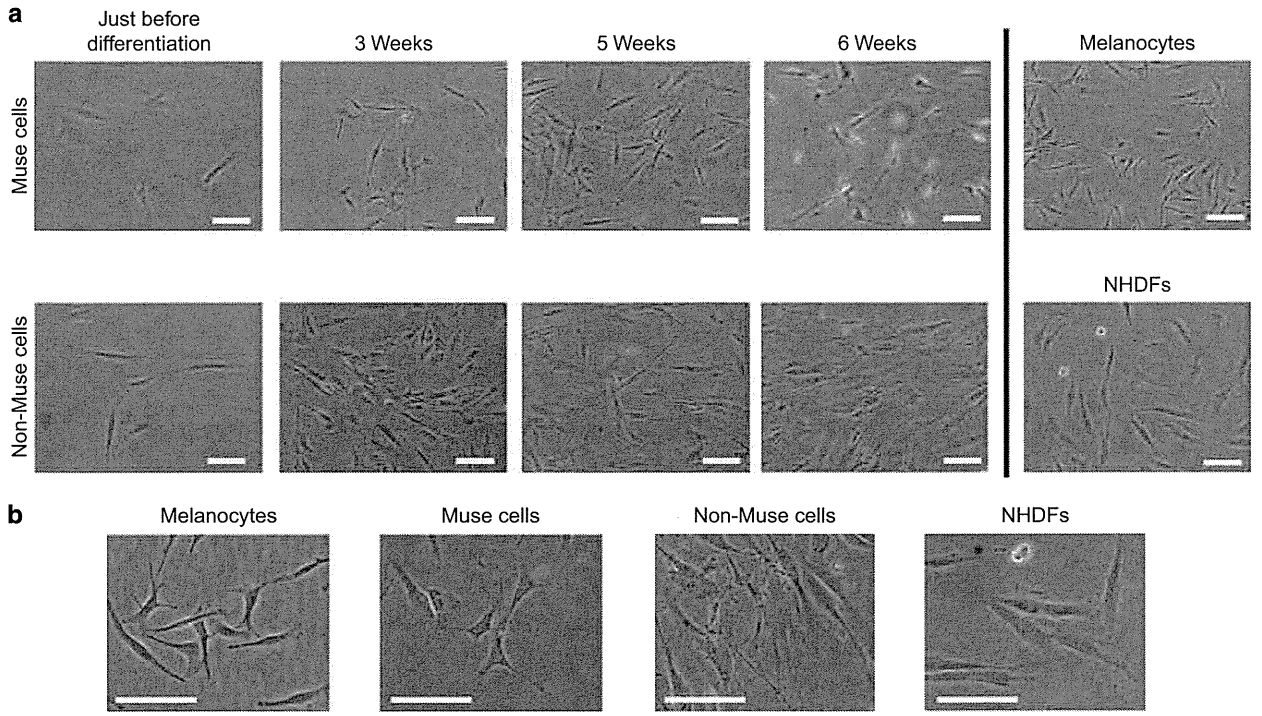

Figure 2. Morphology of Muse (multilineage-differentiating stress-enduring) cells and non-Muse cells after differentiation. (**a**) Microscopic images of Muse cells and non-Muse cells before and 3, 5, and 6 weeks after the differentiation. Microscopic images of naive normal human dermal fibroblasts (NHDFs) and human melanocytes are also provided. Scale bars = 100 μm. (**b**) High magnification of Muse cells and non-Muse cells at 6 weeks after differentiation. Normal human melanocytes and NHDFs are also shown.

media were not superior to the medium with 10 factors in melanocyte induction (Figure 4b). Muse cells cultured in media 1 and 2 expressed only MITF and/or KIT. In media 3, 4, and 7, Muse cells expressed several melanocyte-related markers but not tyrosinase.

Generation of 3D cultured skin using Muse melanocytes

We tried to construct a three-dimensional (3D) cultured skin using Muse melanocytes, as well as other cell types. A gel layer was created comprising collagen type 1 and NHDF to mimic the dermis. For construction of the epidermis, either culture 1, comprising keratinocytes + Muse melanocytes, or culture 2, comprising keratinocytes only, or culture 3, comprising keratinocytes + human melanocytes, or culture 4, comprising keratinocytes + non–Muse cell-derived cells, was seeded onto the gel layer. After 15 days, pigmented cells were observed in the basal layer of the epidermis of cultures 1 and 3 (Figure 5a and b). Because culture 1 comprised human keratinocytes and Muse melanocytes, and keratinocytes do not normally produce melanin, the cells producing melanin in culture 1 were considered to be Muse melanocytes (Figure 5b). In addition, cells positive for MITF, tyrosinase, TRP-1, gp100, and S100 were identified in both cultures 1 and 3, and the Fontana–Masson staining revealed the presence of melanin in the epidermis of both cultures (Figure 5c). In contrast, no pigmented cells or cells positive for melanocyte-related markers and the Fontana–Masson staining were observed in the cultured skin from cultures 2 and 4 (Figure 5a and c). The spontaneous differentiation potential of Muse cells in the 3D cultured skin was also examined. We mixed green fluorescent protein (GFP)–labeled undifferentiated Muse cells (naive Muse cells) with keratinocytes to construct the epidermis of the 3D cultured skin. After 15 days, GFP-positive naive Muse cells were identified in the epidermis but none of them expressed melanocyte markers S100, TRP-1, or tyrosinase (Supplementary Figure S1 online). This result indicated that naive Muse cells do not spontaneously differentiate into melanocytes even if they are integrated into the epidermal layer of 3D cultured skin.

As some groups reported that the 3D cultured human skin model reflects the physiological situation of human melanocytes in human skin more accurately than the experiment using mouse skin (Haake and Scott, 1991; Meier *et al.*, 2000), we used 3D cultured skin to evaluate the migration potential of naive Muse cells and Muse melanocytes. GFP-positive naive Muse cells or Muse melanocytes mixed with NHDF were embedded into the dermal equivalent of 3D cultured skins and then seeded human keratinocytes only on the top of the dermal equivalent. After 15 days, GFP-labeled naive Muse cells were detected in the epidermis of 3D cultured skin (Supplementary Figure S2a online), although they did not express S100, TRP-1, or tyrosinase, as stated above (Supplementary Figure S1 online). Some of the Muse melanocytes migrated from the dermal equivalent, integrated

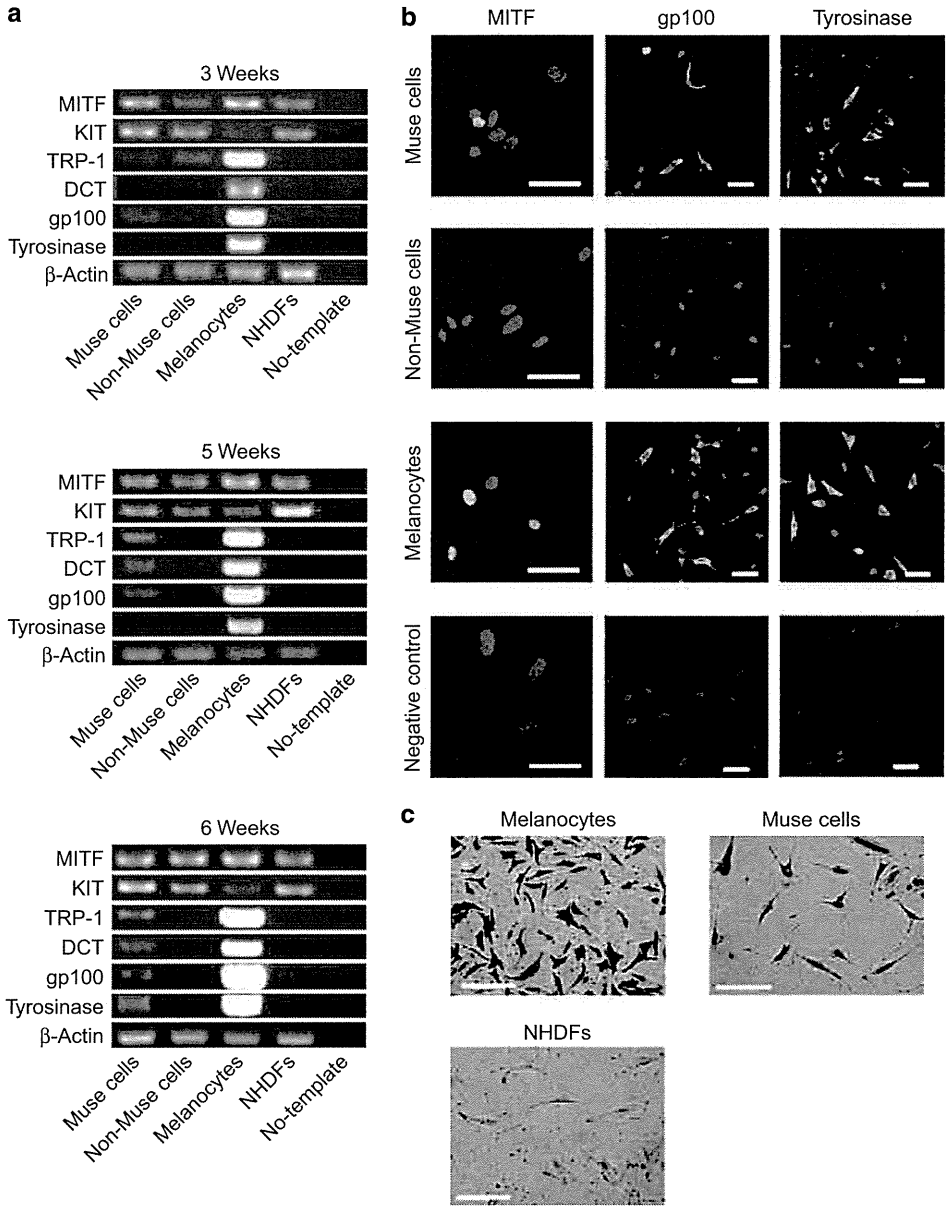

Figure 3. Characterization of Muse (multilineage-differentiating stress-enduring) melanocytes. (**a**) Reverse transcription–PCR (RT–PCR) analysis of microphthalmia-associated transcription factor (MITF), KIT, tyrosinase-related protein 1 (TRP-1), dopachrome tautomerase (DCT), gp100, and tyrosinase at 3, 5, and 6 weeks of differentiation in both Muse and non-Muse cells. The positive control was human melanocytes and the negative controls were naive normal human dermal fibroblasts (NHDFs) and no-template. (**b**) Immunocytochemical analysis of the melanocyte markers MITF, gp100, and tyrosinase in Muse and non-Muse cells at 6 weeks after differentiation. The positive control was human melanocytes and the negative control was naive Muse cells without primary antibody. Scale bars = 50 μm. (**c**) The 3,4-dihydroxy-L-phenylalanine (L-DOPA) reaction assay of Muse melanocytes (6 weeks), human melanocytes, and naive NHDFs. The pigmented cells are L-DOPA-positive cells. Scale bars = 100 μm.

into the epidermal layer, and expressed S100 and TRP-1 (Supplementary Figure S2b online), showing that Muse melanocytes have the potential of migrating into the epidermis where human melanocytes normally reside.

Functional evaluation of Muse melanocytes *in vivo*

To investigate whether Muse melanocytes can survive and maintain their melanocyte functions for a certain period of time *in vivo*, we transplanted 3D cultured skin containing Muse melanocytes onto the back skin of severe combined immunodeficient mice. The 3D cultured skin containing human melanocytes and 3D cultured skin containing only keratinocytes were transplanted as positive and negative controls, respectively. At 10 days after transplantation of the skin containing human melanocytes, some melanocytes were histologically detected in the basal layer of the graft

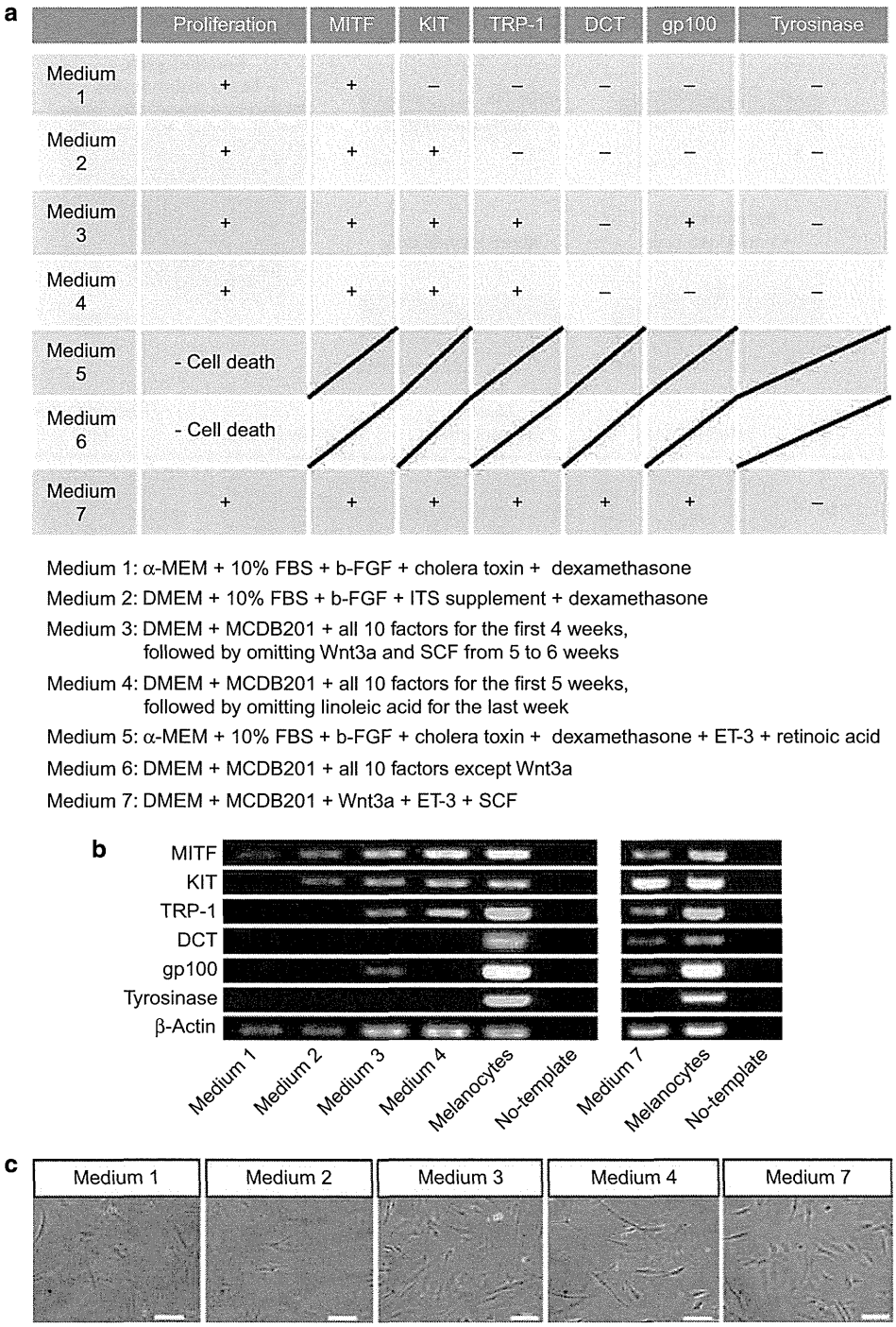

Figure 4. Effect of factors on melanocyte differentiation. (**a**) Summary of the proliferating capacity and melanocyte marker expression of Muse (multilineage-differentiating stress-enduring) cells cultured in seven different media. (**b**) Reverse transcription–PCR (RT–PCR) for microphthalmia-associated transcription factor (MITF), KIT, tyrosinase-related protein 1 (TRP-1), dopachrome tautomerase (DCT), gp100, and tyrosinase in Muse cells at 6 weeks of culture in five different media. The positive control was human melanocytes and the negative control was no-template. (**c**) Morphology of Muse cells in five different media at 6 weeks of culture. Scale bars = 100 μm. FBS, fetal bovine serum; b-FGF, basic fibroblast growth factor; ET-3, endothelin 3; ITS, insulin–transferrin–selenium; SCF, stem cell factor.

(Figure 6a and b). In the negative control, the skin graft did not appear pigmented, and no pigmented cells were observed histologically. Histologic evaluation revealed that skin grafts with Muse melanocytes contained Muse melanocytes located in the basal layer that were brown in color (Figure 6b), and immunohistochemical analysis revealed that they were positive for MITF, tyrosinase, TRP-1, gp100, and S100, the same as grafted human melanocytes (Figure 6c). Furthermore, Muse

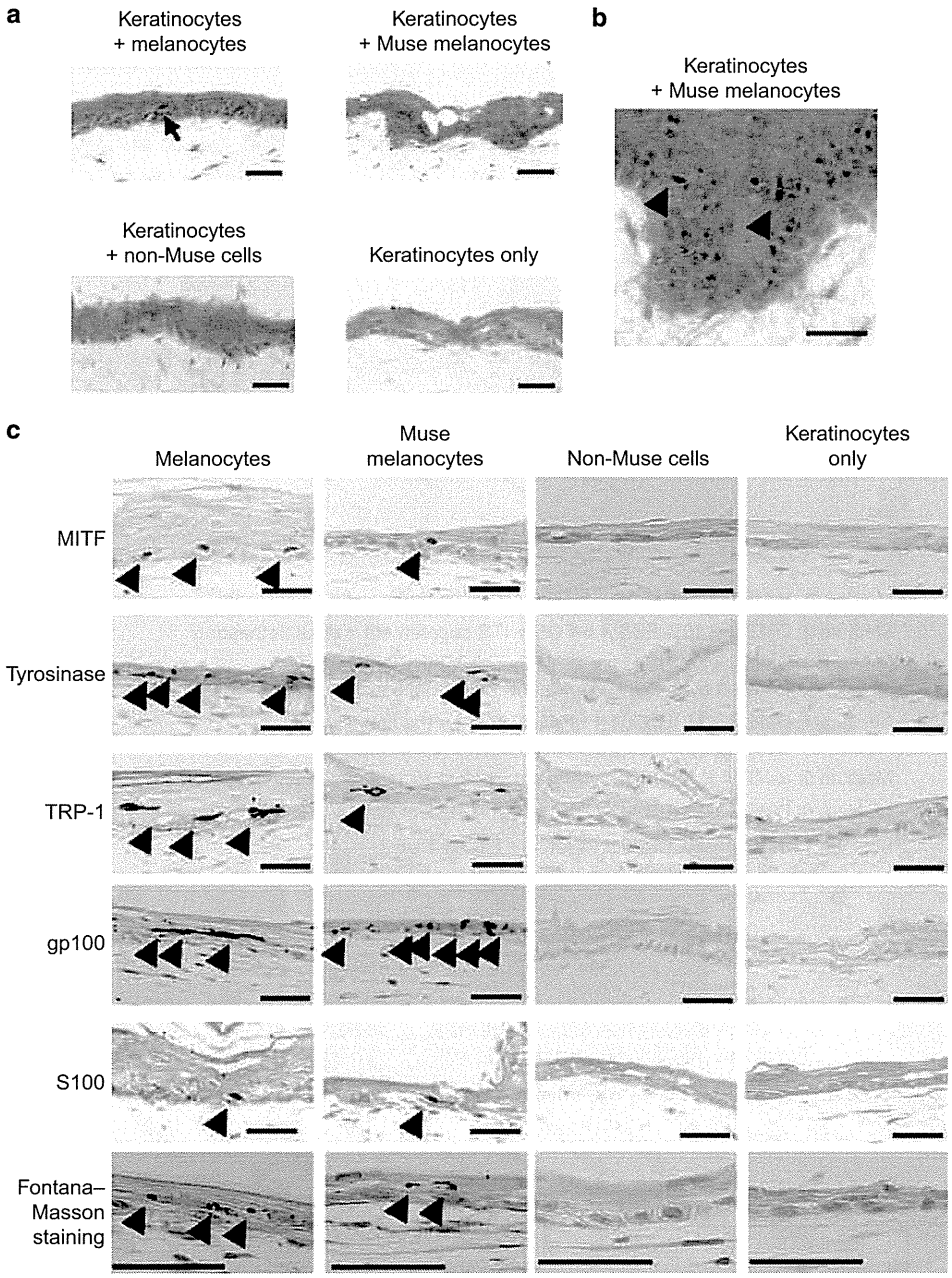

Figure 5. Histologic analysis of three-dimensional (3D) cultured skin. (**a**) Hematoxylin and eosin (H&E) staining of 3D cultured skin containing human melanocytes, Muse (multilineage-differentiating stress-enduring) melanocytes, non-Muse cells, and keratinocytes alone. (**b**) H&E staining of the 3D cultured skin containing Muse melanocytes (arrowheads indicate Muse melanocytes). (**c**) Immunohistochemical analysis of microphthalmia-associated transcription factor (MITF), tyrosinase, tyrosinase-related protein 1 (TRP-1), gp100, and S-100, and the Fontana–Masson staining of the 3D cultured skin. Scale bars = 50 μm.

melanocytes and the neighboring keratinocytes were positive for Fontana–Masson staining, as seen in human melanocytes (Figure 6c). Following transplantation of 3D cultured skin containing GFP-labeled Muse melanocytes, GFP-positive Muse melanocytes were confirmed to be located within the grafted skin, demonstrating that these GFP-positive cells were transplanted cells and not derived from the host (Figure 6d). These findings indicated that Muse melanocytes homed to the basal layer of the epidermis, produced melanin, and delivered it to the neighboring keratinocytes *in vivo*. The negative control, skin graft with keratinocytes only, was negative for all melanocyte-related markers and for the Fontana–Masson staining (Figure 6c).

We performed double staining for the melanocyte marker S100 and the proliferative marker Ki-67 to investigate the proliferation capacity of Muse melanocytes; 9.5% of Muse melanocytes expressed both Ki-67 and S100 (Supplementary Figure S3 online).

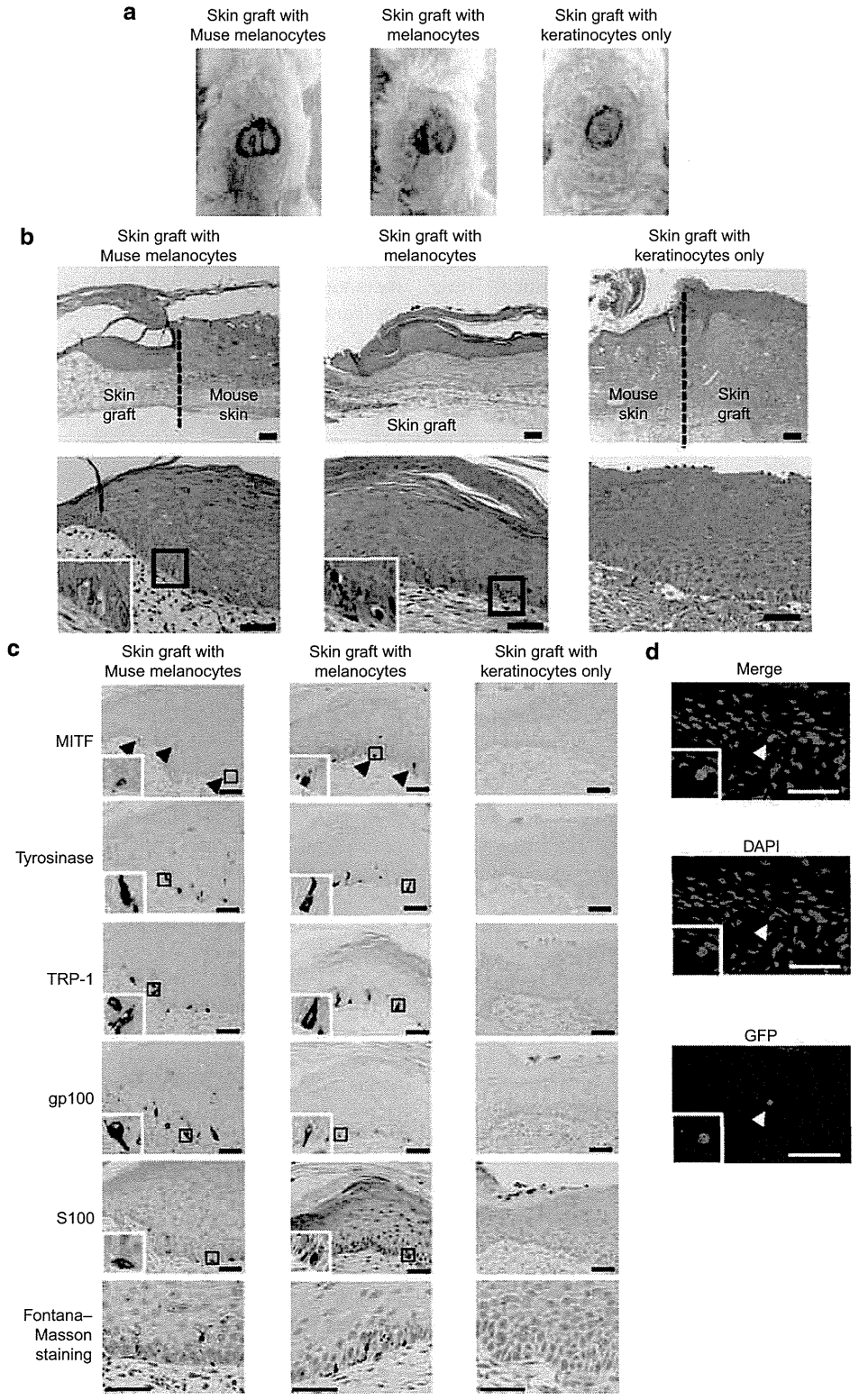

Figure 6. Functional characterization of Muse (multilineage-differentiating stress-enduring) melanocytes after transplantation into the back skin of severe combined immunodeficient (SCID) mouse. (**a**) Macroscopic observation of skin grafts containing Muse melanocytes, human melanocytes, and keratinocytes only 10 days after transplantation. (**b**) Hematoxylin and eosin staining of each skin graft. Scale bars = 100 μm (upper panels) and 50 μm (lower panels). (**c**) Immunohistochemical analysis of microphthalmia-associated transcription factor (MITF), tyrosinase, tyrosinase-related protein 1 (TRP-1), gp100, S100, and the Fontana–Masson staining in the skin grafts. (**d**) Localization of Muse melanocytes labeled with green fluorescent protein (GFP) detected by anti-GFP antibody and Alexa-568 (in red) was observed (arrow). Scale bars = 50 μm. DAPI, 4′,6-diamidino-2-phenylindole.

DISCUSSION

The findings of this study revealed that a specific type of stem cell, Muse cells, among NHDF can be readily reprogrammed to functional melanocytes by using a specific combination of factors and cytokines, whereas other cells among NHDF, non-Muse cells, cannot. Muse melanocytes expressed melanocyte markers during immunocytochemical analysis and RT–PCR showed a positive reaction to L-DOPA *in vitro*, could grow in 3D cultured skin, survived *in vivo*, expressed melanocyte markers, and produced melanin after transplantation to the back skin of severe combined immunodeficient mice. Thus, Muse melanocytes are considered to be equivalent to melanocytes.

DPSCs, a MSC type, are reported to differentiate into melanocytes (Stevens *et al.*, 2008; Paino *et al.*, 2010). Stevens *et al.* (2008) successfully induced cells that expressed the melanocyte marker, Mart-1 (melanoma antigen recognized by T-cells 1), from CD34(−)/CD271(+) DPSCs. Although Muse cells in NHDF are also CD34(−), they might be distinct from dental pulp cells because NHDF-derived Muse cells are negative for CD271, as reported previously. Whether or not Muse cells are contained in the dental pulp mesenchymal cells is an interesting question that should be examined in future studies. Paino *et al.* (2010) reported that DPSCs spontaneously differentiate into melanocytes without any stimulation. The spontaneously differentiated cells express DCT, TRP-1, and Mart-1 and are positive for the L-DOPA reaction assay. Although spontaneous differentiation is indeed attractive, more than 150 days were required. Compared with melanocytes derived from DPSCs, Muse cells could differentiate into melanocytes within 6 weeks and expressed tyrosinase, the essential enzyme for producing melanin. For these reasons, Muse melanocytes are expected to be practical for clinical use.

Several groups have already reported that melanocytes can be induced from ES cells and iPS cells (Yamane *et al.*, 1999; Fang *et al.*, 2006; Motohashi *et al.*, 2006; Nissan *et al.*, 2011; Ohta *et al.*, 2011; Yang *et al.*, 2011). These melanocytes, like Muse melanocytes, express several melanocyte-related markers containing tyrosinase and produce melanin in 3D cultured skin. The techniques for inducing melanocytes from Muse cells are important in relation to the clinical application. ES cells and iPS cells increase the risk for tumorigenesis (Okita *et al.*, 2007; Fong *et al.*, 2010; Ben-David *et al.*, 2011; Goldring *et al.*, 2011), whereas MSCs, which contain Muse cells, have a low risk of tumorigenesis and have already been applied to patients in many clinical trials (Kuroda *et al.*, 2011). Because ES cells are obtained from fertilized eggs, treating ES cells requires much more effort and poses more ethical problems (Knoppers *et al.*, 2009; Manzar *et al.*, 2011). The iPS cells are obtained from somatic cells such as fibroblasts, and hence the ethical problems are avoided, but they require artificial gene transduction to generate pluripotent stem cells (Takahashi *et al.*, 2006, 2007). Muse cells, in contrast, normally reside in accessible mesenchymal tissue such as the dermis and in commercially available fibroblasts, and hence that they are an attractive cell source for clinical and industrial uses. In addition, Muse cells are easily isolated from mesenchymal cells by simple labeling with SSEA-3 in a cell-sorting system, and this is beneficial particularly for industrial use. As Muse cells can be obtained from accessible mesenchymal tissues, autologous transplantation of Muse melanocytes can also be expected.

Human melanocyte stem cells are known to reside in hair follicles, have self-renewal capacity, and have a role in maintaining the number of melanocytes in the epidermis. Both DCT and PAX3 are known as markers of melanocyte stem cells. We have demonstrated DCT expression of Muse melanocytes at the mRNA level. In order to investigate the proliferative capacity of Muse melanocytes, we examined the Ki-67 expression of Muse melanocytes (Supplementary Figure S3 online). The result showed that 9.5% of Muse melanocytes expressed Ki-67. In addition, these Ki-67-positive cells were also positive for S-100, a marker for melanocytes. Although in-depth analysis is needed to confirm the self-renewal ability of Muse cells, these results indirectly suggested the self-renewal capacity of Muse melanocytes after transplantation.

The Wnt3a, ET-3, SCF, basic fibroblast growth factor, and cAMP inducers (cholera toxin and 12-*O*-tetradecanoyl-phorbol 13-acetate) used in the differentiation medium are known to promote the expression of transcription factors PAX3, SOX10, CREB, and LEF1 through intracellular signaling (Steingrimsson *et al.*, 2004; Kondo *et al.*, 2011; Dong *et al.*, 2012). These four transcription factors regulate the promoter of MITF-M, which is one of the MITF variants specific for melanocytes and has a crucial role in melanocyte differentiation, proliferation, survival, and melanogenesis. In view of this, Wnt3a, ET-3, SCF, basic fibroblast growth factor, and cAMP inducers in the differentiation medium are considered to induce melanocyte-related factors in Muse cells through MITF-M activation. Ascorbic acid is known to stimulate the activity and synthesis of tyrosinase (Lee SA *et al.*, 2011). Dexamethasone was recently reported to promote the generation of melanocytic cells from mouse ES cells (Yamane *et al.*, 1999). Both linoleic acid and insulin–transferrin–selenium supplement were used as supplemental factors in low serum medium. Collectively, it is supposed that these factors cooperatively worked on the efficient induction of Muse cells into melanocytes. To investigate the essential factors for melanocyte reprogramming, we created seven combinations of factors based on articles reporting melanocyte induction from various stem cells (Yamane *et al.*, 1999; Motohashi *et al.*, 2007; Paino *et al.*, 2010). Fang *et al.* (2006) described that a combination of three factors (Wnt3a, ET-3, and SCF) is sufficient to induce melanocytes from pluripotent stem cells. In our experiment, when Muse cells were cultured in medium lacking any of those three factors, they expressed very few melanocyte-related markers and their morphology was different from that of authentic melanocytes. In addition, Muse cells cultured in medium containing only those three factors expressed MITF, KIT, TRP-1, DCT, and gp100, but not tyrosinase, suggesting that although these three factors are necessary for differentiation into melanocytes, Muse cells need additional differentiation-enhancing factors such as cholera toxin, 12-*O*-tetradecanoyl-phorbol 13-acetate, and linoleic acid in order to become mature melanocytes.

MATERIALS AND METHODS

Melanocyte induction

After sorting, Muse cells and non-Muse cells were seeded separately at a density of 10,000 cells per six-well plate and cultured for 1 day in α-MEM (Invitrogen, Carlsbad, CA). The cells were then cultured in differentiation medium containing 0.05 M dexamethasone (Sigma-Aldrich, St Louis, MO), 1 × insulin–transferrin–selenium (Invitrogen), 1 mg ml^{-1} linoleic acid–BSA (Sigma-Aldrich), 30% low-glucose DMEM (Invitrogen), 20% MCDB-201 medium (Sigma-Aldrich), 10^{-4} M L-ascorbic acid (Sigma-Aldrich), 50% DMEM conditioned by L-Wnt3a cells (ATCC, Manassas, VA), 50 ng ml^{-1} SCF (R&D Systems, Minneapolis, MN), 10 nM ET-3 (Sigma-Aldrich), 20 pM cholera toxin (Wako, Osaka, Japan), 50 nM 12-*O*-tetradecanoylphorbol 13-acetate (Sigma-Aldrich), and 4 ng ml^{-1} basic fibroblast growth factor (Wako). All chemical reagents were treated according to the product information sheets. Cells were maintained in this differentiation medium for 6 weeks. The medium was changed every 2 days. Cultures were passaged when cells reached 50 to 80% confluency. Melanocyte induction from both Muse and non-Muse cells was repeated at least three times.

The methods for cell culture, FACS, evaluation of Muse cell pluripotency, generating Wnt3a-conditioned medium, RT–PCR, immunocytochemistry, L-DOPA reaction assay, immunohistochemistry, the Fontana–Masson stain, generation of 3D cultured skin *in vitro*, and skin transplantation are described in Supplementary Materials Online.

CONFLICT OF INTEREST

The authors state no conflict of interest.

ACKNOWLEDGMENTS

We thank Drs Masaki Kitada and Hideo Akashi for valuable discussion. This work was supported by the Japan New Energy and Industrial Technology Development Organization.

SUPPLEMENTARY MATERIAL

Supplementary material is linked to the online version of the paper at http://www.nature.com/jid

REFERENCES

Alikhan A, Felsten LM, Daly M *et al.* (2011) Vitiligo: a comprehensive overview Part I. Introduction, epidemiology, quality of life, diagnosis, differential diagnosis, associations, histopathology, etiology, and work-up. *J Am Acad Dermatol* 65:473–91

Ben-David U, Benvenisty N (2011) The tumorigenicity of human embryonic and induced pluripotent stem cells. *Nat Rev Cancer* 11:268–77

Dezawa M, Kanno H, Hoshino M *et al.* (2004) Specific induction of neuronal cells from bone marrow stromal cells and application for autologous transplantation. *J Clin Invest* 113:1701–10

Dong L, Li Y, Cao J *et al.* (2012) FGF2 regulates melanocytes viability through the STAT3-transactivated PAX3 transcription. *Cell Death Differ* 19:616–22

Fang D, Leishear K, Nguyen TK *et al.* (2006) Defining the conditions for the generation of melanocytes from human embryonic stem cells. *Stem Cells* 24:1668–77

Felsten LM, Alikhan A, Petronic-Rosic V (2011) Vitiligo: a comprehensive overview Part II: treatment options and approach to treatment. *J Am Acad Dermatol* 65:493–514

Fioramonti P, Onesti MG, Marchese C *et al.* (2012) Autologous cultured melanocytes in vitiligo treatment comparison of two techniques to prepare the recipient site: erbium-doped yttrium aluminum garnet laser versus dermabrasion. *Dermatol Surg* 38:809–12

Fong CY, Gauthaman K, Bongso A (2010) Teratomas from pluripotent stem cells: a clinical hurdle. *J Cell Biochem* 111:769–81

Goldring CE, Duffy PA, Benvenisty N *et al.* (2011) Assessing the safety of stem cell therapeutics. *Cell Stem Cell* 8:618–28

Haake AR, Scott GA (1991) Physiologic distribution and differentiation of melanocytes in human fetal and neonatal skin equivalents. *J Invest Dermatol* 96:71–7

Hare JM, Traverse JH, Henry TD *et al.* (2009) A randomized, double-blind, placebo-controlled, dose-escalation study of intravenous adult human mesenchymal stem cells (prochymal) after acute myocardial infarction. *J Am Coll Cardiol* 54:2277–86

Jiang R, Han Z, Zhuo G *et al.* (2011) Transplantation of placenta-derived mesenchymal stem cells in type 2 diabetes: a pilot study. *Front Med* 5: 94–100

Knoppers BM, Bordet S, Isasi R (2009) The human embryo: ethical and legal aspects. *Methods Mol Biol* 550:281–305

Kondo T, Hearing VJ (2011) Update on the regulation of mammalian melanocyte function and skin pigmentation. *Expert Rev Dermatol* 6: 97–108

Kuroda Y, Kitada M, Wakao S *et al.* (2010) Unique multipotent cells in adult human mesenchymal cell populations. *Proc Natl Acad Sci USA* 107:8639–43

Kuroda Y, Kitada M, Wakao S *et al.* (2011) Bone marrow mesenchymal cells: how do they contribute to tissue repair and are they really stem cells? *Arch Immunol Ther Exp* 59:369–78

Lee SA, Son YO, Kook SH *et al.* (2011) Ascorbic acid increases the activity and synthesis of tyrosinase in B16F10 cells through activation of p38 mitogen-activated protein kinase. *Arch Dermatol Res* 303:669–78

Mabula JB, Chalya PL, McHembe MD *et al.* (2012) Skin cancers among Albinos at a University teaching hospital in Northwestern Tanzania: a retrospective review of 64 cases. *BMC Dermatol* 12:5

Macchiarini P, Jungebluth P, Go T *et al.* (2008) Clinical transplantation of a tissue-engineered airway. *Lancet* 372:2023–30

Manzar N, Manzar B, Hussain N *et al.* (2011) The ethical dilemma of embryonic stem cell research. *Sci Eng Ethics* 19:97–106

Meier F, Nesbit M, Hsu MY *et al.* (2000) Human melanoma progression in skin reconstructs: biological significance of bFGF. *Am J Pathol* 156:193–200

Motohashi T, Aoki H, Chiba K *et al.* (2007) Multipotent cell fate of neural crest-like cells derived from embryonic stem cells. *Stem Cells* 25:402–10

Motohashi T, Aoki H, Yoshimura N *et al.* (2006) Induction of melanocytes from embryonic stem cells and their therapeutic potential. *Pigment Cell Res* 19:284–9

Nissan X, Larribere L, Saidani M *et al.* (2011) Functional melanocytes derived from human pluripotent stem cells engraft into pluristratified epidermis. *Proc Natl Acad Sci USA* 108:14861–6

Ohta S, Imaizumi Y, Okada Y *et al.* (2011) Generation of human melanocytes from induced pluripotent stem cells. *PloS One* 6:e16182

Okita K, Ichisaka T, Yamanaka S (2007) Generation of germline-competent induced pluripotent stem cells. *Nature* 448:313–7

Paino F, Ricci G, De Rosa A *et al.* (2010) Ecto-mesenchymal stem cells from dental pulp are committed to differentiate into active melanocytes. *Eur Cell Mater* 20:295–305

Phinney DG, Prockop DJ (2007) Concise review: mesenchymal stem/multipotent stromal cells: the state of transdifferentiation and modes of tissue repair–current views. *Stem Cells* 25:2896–902

Pittenger MF, Mackay AM, Beck SC *et al.* (1999) Multilineage potential of adult human mesenchymal stem cells. *Science* 284:143–7

Sakaida I, Terai S, Yamamoto N *et al.* (2004) Transplantation of bone marrow cells reduces CCl4-induced liver fibrosis in mice. *Hepatology* 40:1304–11

Slominski A, Tobin DJ, Shibahara S *et al.* (2004) Melanin pigmentation in mammalian skin and its hormonal regulation. *Physiol Rev* 84:1155–228

Sng J, Lufkin T (2012) Emerging stem cell therapies: treatment, safety, and biology. *Stem Cells Int* 2012:521343

Steingrimsson E, Copeland NG, Jenkins NA (2004) Melanocytes and the microphthalmia transcription factor network. *Annu Rev Genet* 38:365–411

Stevens A, Zuliani T, Olejnik C *et al.* (2008) Human dental pulp stem cells differentiate into neural crest-derived melanocytes and have label-retaining and sphere-forming abilities. *Stem Cells Dev* 17:1175–84

Takahashi K, Tanabe K, Ohnuki M *et al.* (2007) Induction of pluripotent stem cells from adult human fibroblasts by defined factors. *Cell* 131:861–72

Takahashi K, Yamanaka S (2006) Induction of pluripotent stem cells from mouse embryonic and adult fibroblast cultures by defined factors. *Cell* 126:663–76

Toma JG, McKenzie IA, Bagli D *et al.* (2005) Isolation and characterization of multipotent skin-derived precursors from human skin. *Stem Cells* 23: 727–37

van Geel N, Ongenae K, Naeyaert JM (2001) Surgical techniques for vitiligo: a review. *Dermatology* 202:162–6

Wakao S, Kitada M, Kuroda Y *et al.* (2011) Multilineage-differentiating stress-enduring (Muse) cells are a primary source of induced pluripotent stem cells in human fibroblasts. *Proc Natl Acad Sci USA* 108:9875–80

Yamane T, Hayashi S, Mizoguchi M *et al.* (1999) Derivation of melanocytes from embryonic stem cells in culture. *Dev Dyn* 216:450–8

Yang R, Jiang M, Kumar SM *et al.* (2011) Generation of melanocytes from induced pluripotent stem cells. *J Invest Dermatol* 131: 2458–66

Research article

Autologous mesenchymal stem cell–derived dopaminergic neurons function in parkinsonian macaques

Takuya Hayashi,[1,2,3,4] Shohei Wakao,[5] Masaaki Kitada,[5] Takayuki Ose,[1] Hiroshi Watabe,[1,6] Yasumasa Kuroda,[7] Kanae Mitsunaga,[5] Dai Matsuse,[5] Taeko Shigemoto,[5] Akihito Ito,[8] Hironobu Ikeda,[8] Hidenao Fukuyama,[3] Hirotaka Onoe,[1] Yasuhiko Tabata,[9] and Mari Dezawa[5,7]

[1]Functional Probe Research Laboratory, Center for Molecular Imaging Science, RIKEN, Kobe, Japan. [2]National Cerebral Cardiovascular Center Research Institute, Osaka, Japan. [3]Human Brain Research Center, Graduate School of Medicine, and [4]Center for iPS Cell Research and Application, Kyoto University, Kyoto, Japan. [5]Department of Stem Cell Biology and Histology, Tohoku University Graduate School of Medicine, Sendai, Miyagi, Japan. [6]Faculty of Molecular Imaging in Medicine, Osaka University Graduate School of Medicine, Suita, Osaka, Japan. [7]Department of Anatomy and Anthropology, Tohoku University Graduate School of Medicine, Sendai, Miyagi, Japan. [8]Shiga Research Institute, Nissei Bilis Co. Ltd., Koga, Shiga, Japan. [9]Department of Biomaterials, Field of Tissue Engineering, Institute for Frontier Medical Sciences, Kyoto University, Kyoto, Japan.

A cell-based therapy for the replacement of dopaminergic neurons has been a long-term goal in Parkinson's disease research. Here, we show that autologous engraftment of A9 dopaminergic neuron-like cells induced from mesenchymal stem cells (MSCs) leads to long-term survival of the cells and restoration of motor function in hemiparkinsonian macaques. Differentiated MSCs expressed markers of A9 dopaminergic neurons and released dopamine after depolarization in vitro. The differentiated autologous cells were engrafted in the affected portion of the striatum. Animals that received transplants showed modest and gradual improvements in motor behaviors. Positron emission tomography (PET) using [^{11}C]-CFT, a ligand for the dopamine transporter (DAT), revealed a dramatic increase in DAT expression, with a subsequent exponential decline over a period of 7 months. Kinetic analysis of the PET findings revealed that DAT expression remained above baseline levels for over 7 months. Immunohistochemical evaluations at 9 months consistently demonstrated the existence of cells positive for DAT and other A9 dopaminergic neuron markers in the engrafted striatum. These data suggest that transplantation of differentiated autologous MSCs may represent a safe and effective cell therapy for Parkinson's disease.

Introduction

Cell-based therapies are expected to replace the missing dopaminergic neurons and to restore the motor function in patients with Parkinson's disease (PD) (1). Early studies on cell-based therapies used fetal midbrain tissue containing dopaminergic neurons as a cell source and suggested potential therapeutic effects in PD (for review, see refs. 2, 3). However, limited availability and ethical considerations relating to the use of fetuses pose limitations for practical use. Bone marrow–derived mesenchymal stem cells (MSCs), a type of adult stem cells, have trophic effects (4) and a differentiation spectrum that crosses oligolineage boundaries (5), offering the potential for use in autologous cell therapy, with low risk of tumorigenesis (6). The MSCs have been already tested for cell therapy in PD model rodents (7–9) and even in patients with PD (10). However, they have shown poor performance for restoration of motor function, potentially due to limited spontaneous differentiation (11) or facilitated apoptosis (12, 13) of MSCs. Recent studies of fetal midbrain graft have suggested that better outcomes could be obtained if the graft consisted of well-differentiated A9 dopaminergic neurons (14–16), the most severely damaged neuronal type in PD (17). Therefore, differentiation of MSCs into desired cells, such as A9 dopaminergic neurons, would probably provide effective functional restoration in PD.

Recently, it was shown that MSCs could be artificially directed to differentiate into several specialized cell types, including those in nervous tissues (18–21). Previously, we reported that dopamine-producing cells could be induced from MSCs (MSC-DP cells) by introduction of a Notch1 intracellular domain–containing (NICD-containing) plasmid, followed by cytokine stimulation with bFGF, forskolin, ciliary neurotrophic factor (CNTF), and glial cell line–derived neurotrophic factor (GDNF) (20, 21). The differentiated cells were positive for markers of dopaminergic neurons, such as tyrosine hydroxylase (TH) and the dopamine transporter (DAT), and had an ability to release dopamine after depolarization by potassium stimulation. When rat and human MSC-DP cells were transplanted into the striata of PD model rats, integration of TH$^+$ and DAT$^+$ cells and functional recovery in motor behaviors were confirmed (20). Subsequent development of a spermine-pullulan–mediated reverse transfection method allowed us to induce MSC-DP cells more safely and efficiently than before from MSCs of macaque monkeys (21), an animal species frequently used for preclinical trials of PD (22–27).

To test the scalability of MSC-DP cell–based therapy in primates in this study, monkey MSC-DP cells were characterized in detail using specific markers and evaluated for their longitudinal effects after they were engrafted into hemiparkinsonian monkeys using behavioral tests and positron emission tomography (PET). The MSC-DP cells, prepared autologously from the bone marrow of

Authorship note: Takuya Hayashi and Shohei Wakao contributed equally to this work.

Conflict of interest: The authors have declared that no conflict of interest exists.

Citation for this article: *J Clin Invest.* 2013;123(1):272–284. doi:10.1172/JCI62516.

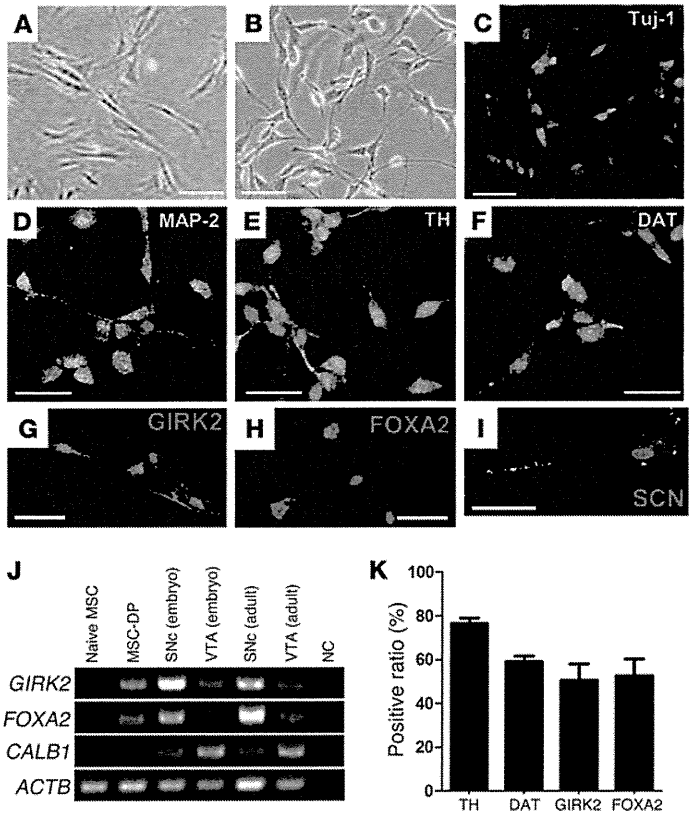

Figure 1

Monkey bone marrow MSCs and MSC-DP cells. (**A**) Morphological changes were evident in cynomolgus naive MSCs (phase-contrast microscopy) and (**B**) MSC-DP cells (phase-contrast microscopy). The MSC-DP cells possessed neurite-like processes. Immunocytochemistry of MSC-DP cells showed that the cells were immunoreactive for the neuronal markers (**C**) Tuj1 and (**D**) MAP-2; for the markers of dopaminergic neurons (**E**) TH, (**F**) DAT, (**G**) GIRK2, and (**H**) FOXA2; and for the marker of neurons, (**I**) sodium channel (SCN). DAPI was used for counterstaining of nuclei. Scale bar: 30 μm. (**J**) Results of RT-PCR in naive MSCs, MSC-DP cells, and tissue samples from the SNc and VTA. Naive MSCs expressed no *GIRK2*, *FOXA2*, and *CALB1* mRNA, while the MSC-DP cells expressed *GIRK2* and *FOXA2* mRNA. SNc tissue samples from an embryo and an adult cynomolgus monkey also contained high levels of *GIRK2* and *FOXA2* mRNA but only low levels of *CALB1* mRNA, while the VTA contained high levels of *CALB1* mRNA and only very low levels of *GIRK2* and *FOXA2* mRNA. NC, negative control. (**K**) Percentages of cells immunoreactive for TH, DAT, GIRK2, and FOXA2 in MSC-DP cells.

each test animal, expressed cell makers not only for antigens that have been previously described (20, 21), such as β tubulin III (Tuj1), microtubule-associated protein 2 (MAP-2), TH, and DAT, but also for those specific to the A9 subtype, namely, G protein–coupled inward rectifying current potassium channel type 2 (GIRK2) (15) and forkhead box protein A2 (FOXA2) (28). The effect of transplantation was evaluated for up to 9 months based on motor behaviors of affected hand movements; PET scans using ^{11}C-CFT, which specifically labels DAT; and postmortem histology. Tumorigenicity was also estimated from the results of blood tests and PET scans. The preclinical data obtained thus may extend the applicability of the current autologous cell system as a therapy for PD.

Results

Evaluation of MSC-DP cells. Cynomolgus monkey MSCs drastically changed their morphology following induction, as reported previously (21): naive MSCs initially showed fibroblast-like mesenchymal cell features (Figure 1A), while induced cells showed a neuron-like morphology with neurite-like processes (Figure 1B). By immunohistochemistry, naive MSCs were negative for neuronal markers, as reported previously (21), but induced cells were positive for neuronal markers, Tuj1 (Figure 1C) and MAP-2 (Figure 1D); dopaminergic neuron markers, TH and DAT (Figure 1, E and F); the A9 dopaminergic neuron marker, GIRK2 (Figure 1G); and a marker of floor plate–derived cells, FOXA2 (Figure 1H). We also confirmed that these cells were positive for sodium channels (Figure 1I), a marker of differentiated neurons.

To confirm whether these cells have an ability to produce and release dopamine, we measured the secretion of dopamine by HPLC. The amount of dopamine in the culture supernatant was measured following application of high K^+ depolarizing stimuli, which resulted in release of 1.04 ± 0.4 pM dopamine per 10^6 cells (Table 1); by contrast, naive cynomolgus monkey MSCs showed no detectable dopamine release. These results are consistent with those of our previous studies: the amount of dopamine release was comparable to the amounts in rats (1.1 pM/10^6 cells) (20) and monkeys (0.9 ± 0.2 pM/10^6 cells) (21).

We further investigated the expression of markers specific for A9 dopamine neurons using RT-PCR. The MSC-DP cells expressed *GIRK2* and *FOXA2* mRNA but not *CALB1* mRNA (*GIRK2*$^+$/*FOXA2*$^+$/*CALB1*$^-$) (Figure 1J). When control tissues obtained from a cynomolgus embryo and an adult animal were analyzed, both showed that the substantia nigra pars compacta (SNc) was strongly positive for GIRK2 and FOXA2 and weakly positive for calbindin, while the ventral tegmental area (VTA) was weakly positive for GIRK2 and FOXA2 but strongly positive for calbindin (Figure 1J). This distinct pattern of GIRK2/FOXA2/calbindin expression in the SNc and VTA is consistent with those reported in other species, including rodents and humans (15, 28, 29). We also evaluated the induction efficiency of MSC-DP cells by quantitative immunocytochemistry. Fifty to seventy-five percent of MSC-DP cells were positive for TH, DAT, GIRK2, and FOXA2 (Figure 1K). These findings indicated that the current method efficiently produced MSC-DP cells from the MSCs, which had properties similar to those of the A9 dopamine neurons in the model species.

Behavioral analysis of motor symptoms. The clinical rating scores (CRSs) for parkinsonian animals are shown in Figure 2A. The CRS revealed a significant interaction effect between groups and time

Table 1
Dopamine-producing capacity of MSC-DP cells and the number of engrafted cells

Animal ID	Dopamine release induced by K^+ (pM/10^6 cells)	No. of engrafted cells (× 10^6 counts)
mon0703	2.6	20.4
mon0705	0.5	9.0
mon0708	0.4	12.0
mon0709	0.8	12.7
mon0710	0.9	18.6

Dopamine release induced by K^+ was measured by HPLC. Animals were from the MSC-DP–engrafted group.

after transplantation (F distribution [$F_{4,32}$] = 3.07, $P < 0.05$). Thus, we further tested for an effect of time, separately in each of the groups in our study (engrafted or sham), by 1-way ANOVA. The CRS in the MSC-DP–engrafted group showed a marginal effect of time ($F_{4,16} = 2.95$, $P = 0.055$). In a post-hoc comparison of scores at each time point after engraftment with those at baseline, significant improvements in the CRS were observed at 8 months after engraftment (Dunnett's multiple comparison, $P < 0.05$). This time effect was not observed in the sham group either by 1-way ANOVA or post-hoc analysis.

Hand-reach scores showed similar time courses (Figure 2B). The scores for the affected hand showed significant group and time interaction ($F_{4,32} = 2.83$, $P < 0.05$). One-way ANOVA for the repeated measures of hand-reach scores for the affected hand of the MSC-DP–engrafted group revealed a significant effect of time ($F_{4,16} = 5.62$, $P < 0.001$). A post-hoc comparison of scores at each time point after engraftment with those at baseline revealed significant improvements in hand-reach scores at 4 months (Dunnett's multiple comparison, $P < 0.05$) and 8 months ($P < 0.01$) after engraftment. This effect of time was not observed in the sham group. Therefore, the CRSs and hand-reach scores suggested that the engraftment of MSC-DP cells modestly improved motor behaviors in parkinsonian animals.

Despite these improvements in MSC-DP–grafted animals, spontaneous activities of animals were not affected by any of group (sham vs. MSC-DP engrafted), time (before engraftment and 4 months and 8 months after engraftment), or interaction among these variables (2-way ANOVA with repeated measures, Supplemental Figure 1; supplemental material available online with this article; doi:10.1172/JCI62516DS1). Animals in the engrafted group tended to show higher spontaneous activities than sham-operated animals at 4 and 8 months after engraftment; however, no statistically significant effect of group was observed at any time point in post-hoc analysis (Bonferroni corrected, $P > 0.05$). Within-subject and between-subject data were highly variable, consistent with a previous report in this type of parkinsonian animal model (30). No dyskinesia-like abnormal movements were observed in any MSC-DP cell–engrafted animals during the observation period.

^{11}C-CFT PET. Voxel-based analysis of ^{11}C-CFT binding potential (BP_{ND}) images disclosed a significant effect of time in a cluster extending into the dorsal posterior putamen in the engrafted group (Figure 3C) (family-wise error rate [FWE] corrected, $P < 0.05$; Table 2). The maximum of this cluster was located ($x = 11.5$ mm, $y = -8.0$ mm, $z = 3.5$ mm) in a standard macaque brain space of the Montreal Neurological Institute (MNI) (31) and was safely within the area targeted when engrafting MSC-DP cells into the striatum (Figure 3A). Using this cluster as a region of interest (ROI), we obtained BP_{ND} values for this ROI across all animals, groups, and time points. The BP_{ND} values obtained are presented in Figure 3D. Two-way ANOVA with repeated measures (Figure 3D) revealed significant effects of an interaction between group and time ($F_{4,24} = 4.3$, $P < 0.01$). Post-hoc analysis showed that the BP_{ND} at 7 days after engraftment was higher than that in the sham-operated group (Bonferroni multiple comparison, $T = 4.56$, $P < 0.001$), as shown in Figure 3D. In particular, animal mon0703, who received the graft with the largest amount of MSC-DP cells (Table 1), showed the highest BP_{ND} (0.59) in the engrafted striatum at 7 days after engraftment, followed by animal mon0710, who showed a BP_{ND} of 0.43 at 7 days after engraftment (Figure 3B).

The time-dependent decline in ^{11}C-CFT binding in the engrafted striatum (Figure 3D) allowed us to analyze the kinetics of ^{11}C-CFT binding in detail. Because recent studies have suggested that MSCs are susceptible to senescent (12) and apoptotic changes (13), we supposed that this decline was due to degeneration of engrafted MSC-DP cells. ^{11}C-CFT binding is known to be correlated with the density of dopamine neurons or terminals rather than any physiological (or functional) variation in dopamine release. The rate of ^{11}C-CFT binding reduction, calculated based on the 1-hit model of neurodegeneration (32), was 0.30 months (~10 days) as a half-life period (Figure 3E). This rate of reduction was slightly slower than that for engrafted naive rodent MSCs (~3 days; Supplemental Figure 2) based on previously described data (13). We further tested whether this degenerative process would affect all grafted cells. The plateau of the 1-hit model was significantly higher than the baseline (before engraftment) ^{11}CFT binding level (baseline $BP_{ND} = 0.087 \pm 0.028$ vs. BP_{ND} at plateau $= 0.17 \pm 0.029$; Welch's corrected $T_{13} = 2.04$, 1-tailed $P < 0.05$), suggesting that a small portion of the grafted MSC-DP cells survive and integrate

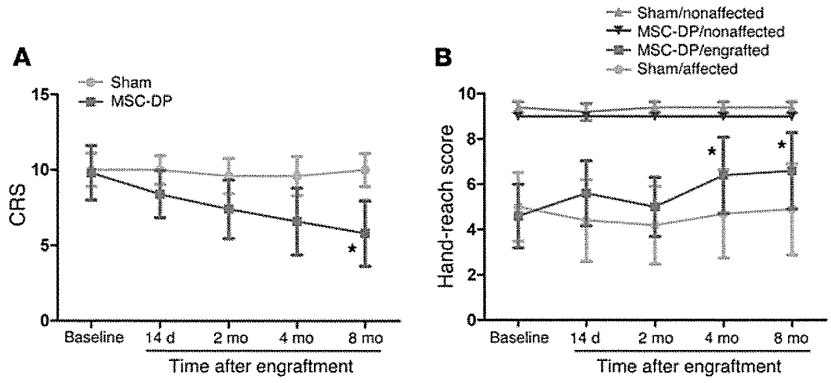

Figure 2
Behavioral assessment. (**A**) CRSs and (**B**) hand-reach scores were plotted against time for MSC-DP cell–engrafted (MSC-DP) and sham-operated (Sham) groups. *$P < 0.05$ compared with baseline in the MSC-DP–engrafted group, Dunnett's multiple comparison test.

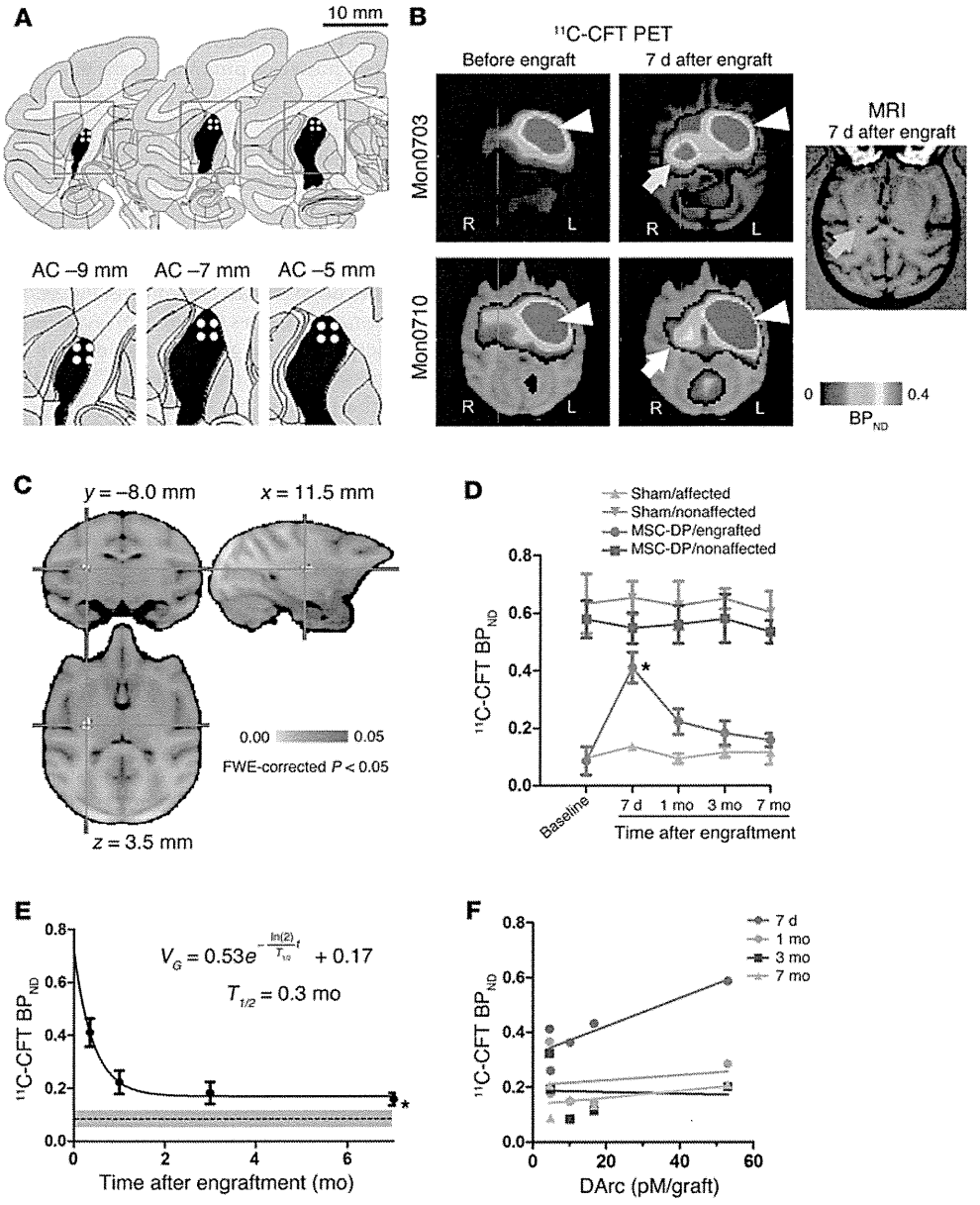

Figure 3

Engrafting and neuroimaging of MSC-DP–engrafted animals. (**A**) Twelve target points (white dots) for engraftment in putamen in the coronal sections of standard space of cynomolgus macaque. Scale bar: 10 mm. (**B**) Representative 11C-CFT PET images of MSC-DP–engrafted animals. Seven days after engraftment (engraft), animal mon0703 showed the highest 11C-CFT BP_{ND} on the MPTP-treated side of striatum (yellow arrow), followed by animal mon0710 (white arrow). Animal mon0710 showed low signal (green arrow) in a T1-weighted MRI after engraftment, which diminished in later scans. Note that the BP_{ND} in the non-MPTP–treated (and nonengrafted) side of striatum was very high (white arrowheads) and not different by engraftments. (**C**) Significant effect of time on 11C-CFT BP_{ND} (P values range from yellow [$P < 0.00$] to red [$P < 0.05$]) overlaid on the study-specific MRI template in MNI space. A cluster with FWE-corrected $P < 0.05$ was located in the dorsal posterior putamen in the engrafted striatum. See also Table 2. (**D**) Time course of 11C-CFT BP_{ND} in the cluster (in **C**) and contralateral equivalent region. *$P < 0.05$ compared with sham, Bonferroni corrected. (**E**) Time course of 11C-CFT BP_{ND} values in the cluster (in **C**), fitted by the 1-hit (exponential) model of neurodegeneration. The dashed line and gray area indicate the mean and SEM for the baseline BP_{ND}. *$P < 0.05$ between the baseline BP_{ND} and the plateau of the fitted model. (**F**) The DArc and the 11C-CFT BP_{ND} values at 7 days and 1, 3, and 7 months after engraftment.

for more than 7 months. This is in contrast to findings in naive MSCs engrafted into rodents, which showed a plateau of the reduction curve returned to the baseline (Supplemental Figure 2), indicating that all naive MSCs may eventually degenerate when transplanted into brain.

We also estimated how the dopamine-releasing capacity (DArc) of grafts related to ^{11}C-CFT binding after engraftment (Figure 3F). The dopamine-releasing capacity was calculated by multiplication of dopamine release by K^+ concentration (pM per 10^6 cells) in vitro, as measured by HPLC, and the total number of cells engrafted in each animal (10^6 cells). This graft DArc (pM/graft) significantly predicted the ^{11}C-CFT BP_{ND} obtained from the cluster of engrafted striatum scanned at 7 days after engraftment (linear regression, $BP_{ND} = 5.1 \times 10^{-3} \times$ DArc + 0.31, $F_{1,3} = 10.3$, $P < 0.05$; Figure 3F) but not those obtained at later time points. Although dopamine release and DAT expression are different measures, both are a common and specific attribute of well-differentiated dopamine neurons (33). Therefore, the findings indicate that the DAT expression at the earliest time point after transplantation is coupled to the dopaminergic capacity of the engrafted cells, while other factors may have degraded this coupling at later time points.

Tests for tumorigenicity and general condition of animals with MSC-DP cell engraftment. There were no abnormal changes in the results of blood tests, including red and white blood cell counts, and blood chemical tests in any of the MSC-DP– and sham-treated animals tested (Supplemental Table 1). There was also no abnormal

Table 2
Voxel-based statistical results of ^{11}C-CFT BP_{ND} in repeated-measure ANOVA

Cluster	No. of voxels	Maximum voxel			
		x (mm)	*y* (mm)	*z* (mm)	F value
Right dorsal posterior striatum	224	11.5	−8.0	3.5	14.6

The location of the maximal voxel is presented in *x*, *y*, and *z* coordinates of the standard anterior-posterior commissural coordinates in MNI space. See Figure 3C for visual presentation of this cluster. FWE-corrected $P < 0.05$.

elevation in the levels of the tumor markers carcinoembryonic antigen (CEA), tissue polypeptide antigen (TPA), sialyl Lewis X antigen (SLX), neuron-specific enolase (NSE), and basic fetoprotein (BFP) (Supplemental Table 2).

^{18}F-FDG PET scans revealed normal uptake of ^{18}F-FDG in the engrafted striatal region of animals in the engrafted group (Figure 4). In MRI scans, 2 animals (mon0710 and mon0049) showed subtle hemorrhagic changes, as suggested by low signals in the engrafted region of the right striatum in T1-weighted MRI images at 7 days after engraftment (Figure 3B); however, no significant signal changes were observed in later MRI scans. Therefore, no enlargement of or tumor formation by the engrafted tissues was suspected, at least at the macroscopic level, up to 8 months after transplantation of MSC-DP cells. These findings were confirmed by histological evaluations, as described below.

Immunohistochemical study. Consistent with the ^{8}F-FDG PET scans and MRI data, no tumor formation was observed in either group by H&E staining (data not shown). We further evaluated the proliferative activity of MSC-DP cells engrafted into the striatum by immunostaining using a Ki-67 antibody. Although, we found a small number of Ki-67$^+$ cells in the MSC-DP cell–engrafted striatum (Figure 4B), the proportion of Ki-67$^+$ cells was <2.5%, and there was no significant difference between MSC-DP cell–engrafted and control striata (Figure 4C). Moreover, the Ki-67$^+$ cells existed solitarily, and none of them formed tumor-like masses (Figure 4B).

We then performed triple staining of striatal sections using markers, including those for A9 and A10 dopaminergic neurons. In the transplanted region of MSC-DP cell–engrafted striata, cells positive for DAT and GIRK2 but not for calbindin were clearly observed (Figure 5, A–F), but such cells were not found in any of sham-operated striata. The staining pattern of A9-type dopaminergic neurons was confirmed by analyzing the midbrain of a normal control adult animal with the same triple staining (Supplemental Figure 3): the A9-type dopaminergic neurons in the SNc showed a pattern of DAPI$^+$/DAT$^+$/GIRK2$^+$/calbindin$^-$ (Supplemental Figure 3A), while the A10-type neurons in the VTA had a pattern of DAPI$^+$/DAT$^+$/GIRK2$^-$/calbindin$^+$ (Supplemental Figure 3B). We also confirmed that most of the DAT$^+$ cells in the engrafted striata were positive for TH (Figure 5, G–J) but not for a glial marker, glial

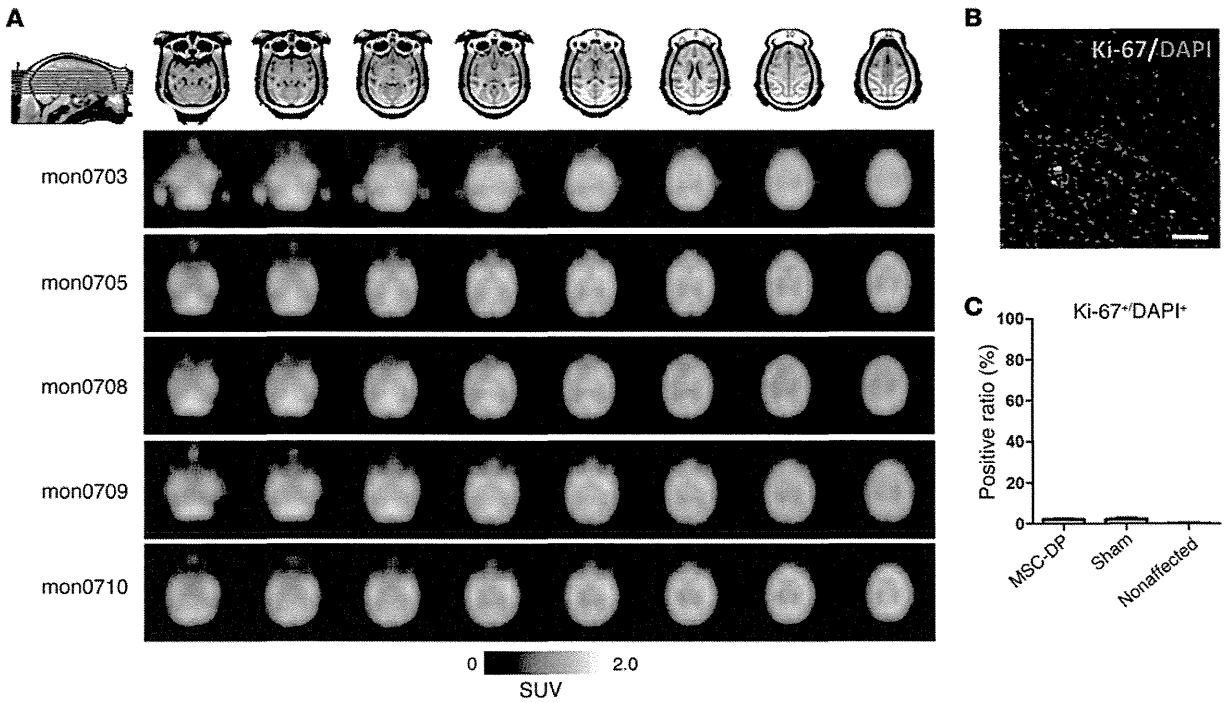

Figure 4
Evaluation of tumorigenicity of MSC-DP–grafted animals. (**A**) SUV images of ^{18}F-FDG PET scans, obtained 8 months after engraftment, are shown for each animal in the engrafted group. No apparently high uptake of ^{18}F-FDG was found in any of MSC-DP cell–engrafted animals. (**B**) Immunostaining with Ki-67 is shown in a section of MSC-DP cell–engrafted striatum. Cells positive for Ki-67 (green) scarcely existed in the dorsal-posterior putamen. Scale bar: 100 μm. (**C**) Quantitative analysis of the ratio of Ki-67$^+$ cells to the total number of cells in 3 groups of striatum (MSC-DP grafted, sham operated, nonaffected). See also Supplemental Tables 1 and 2 for the results of blood tests for biochemical and tumor markers.

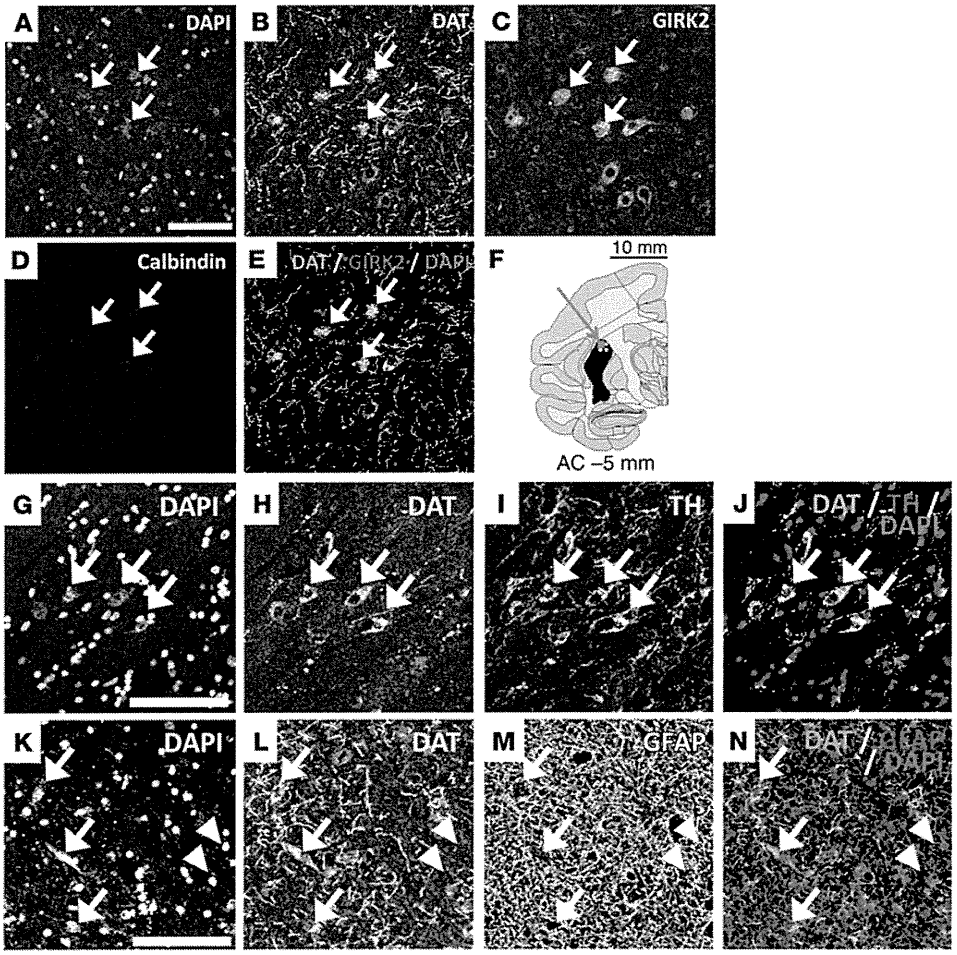

Figure 5
Immunohistochemistry of the MSC-DP–engrafted striatum. In the MSC-DP–grafted striatum, the cell bodies positive for DAT and GIRK2 (arrows in **B** and **C**, respectively) but not for calbindin (arrow in **D**) were found in the area close to the MSC-DP cell–engrafted area (white dots in **F**) in the dorsal posterior putamen. (**A**) DAPI was used for counterstaining of nuclei. (**E**) A merged image for DAT, GIRK2, and DAPI is shown in green, red, and blue, respectively. Most of the DAT$^+$ cells were also positive for TH (arrows in **G**–**J**) but not for GFAP (arrows in **K**–**N**), while the GFAP$^+$ cells with round-shaped nuclei, putative astroglial cells, were not positive for DAT (arrowheads in **K**–**N**). Scale bar: 100 μm (**A**–**E** and **G**–**N**); 100 mm (**F**).

fibrillary acidic protein (GFAP) (Figure 5, K–N). Taken together, these findings indicate that the transplanted MSC-DP cells survived and maintained the characteristics of A9-type dopaminergic neurons for at least 9 months after transplantation.

Quantitative analysis revealed that the number of cells positive for NeuN tended to be higher in the MSC-DP–engrafted striata than in sham and nonaffected (i.e., non–1-methyl-4-phenyl-1,2,3,6-tetrahydoropyridine–treated [non-MPTP–treated]) striata, but no statistically significant differences were found among the 3 groups of striata ($F_{3,112}$ = 1.12, P > 0.05; Figure 6, A and B). The number of TH$^+$ cell bodies in the engrafted region was higher in the MSC-DP group than in the sham and nonaffected groups, with statistical significance ($F_{2,88}$ = 5.99, P < 0.005, Tukey's multiple comparison P < 0.05; Figure 6, A and C). In contrast, the number of TH$^+$ axon terminals was higher in the MSC-DP group than in the sham group, with statistical significance ($F_{2,119}$ = 3.93, P < 0.05, Tukey's multiple comparison P < 0.05; Figure 6, A and D), suggesting that the TH$^+$ cell bodies observed in the engrafted striatal group integrated with host striatal neurons by forming new synaptic connections. Similarly, the number of DAT$^+$ cells was also higher in the MSC-DP group than in the sham and non-affected striatum groups, with statistical significance ($F_{2,74}$ = 16.78, P < 0.0001, Tukey's multiple comparison P < 0.0001; Figure 6, A and E).

Discussion

Early transplantation trials for PD treatments used fetal midbrain tissue as a cell source. Successful results were first reported in studies using macaques in the late 1980s (22–24). Subsequent open-label trials in patients with PD also showed that engrafted fetal neurons can survive, appropriately differentiate, and provide striatal dopamine release as measured by PET and showed clinical improvements (34–36), with only one exception (37). Although later double-blind placebo-controlled trials reported no significant clinical benefits (38, 39), successful cell replacement therapy in PD would probably be achieved with more sophisticated cell preparation, surgical and patient selection procedures (2, 3). In particular, optimization of cell preparation has been an issue when using fetal tissue because of its limited availability and accessibility; thus, there is an urgent need to develop alternative cell sources (40). In addition, recent basic studies based on fetal tissue graft systems have suggested several potential refinements. For example, whether or not the graft contains A9 dopaminergic neurons may be a determinant factor for achieving synaptic formation with host tissues and better behavioral recovery (16). Others have also suggested that expression of DATs in the graft cells alleviates dyskinesias after graft (41). Therefore, proof-of-concept studies using fetal tissue grafts have established the direction of cell-based therapies, including those using stem cells (2, 3, 40). Particular concerns when